Inorganica Chimica Acta 505 (2020) 119463

Contents lists available at ScienceDirect

Inorganica Chimica Acta

journal homepage: www.elsevier.com/locate/ica

Chemistry of vinylidene complexes. XXV. Synthesis and reactions of binuclear μ-vinylidene RePt complexes containing phosphite ligands. Spectroscopic, structural and electrochemical study

Oleg S. Chudin[a], Victor V. Verpekin[a,*], Alexander A. Kondrasenko[a], Galina V. Burmakina[a], Dmitry A. Piryazev[c,d], Alexander D. Vasiliev[b,e], Nina I. Pavlenko[a], Dmitry V. Zimonin[a], Anatoly I. Rubaylo[a,b]

[a] Institute of Chemistry and Chemical Technology SB RAS, Federal Research Center "Krasnoyarsk Science Center SB RAS", Akademgorodok, 50-24, Krasnoyarsk 660036, Russia
[b] Siberian Federal University, Svobodny Prospect, 79, Krasnoyarsk 660041, Russia
[c] Nikolaev Institute of Inorganic Chemistry, Siberian Branch of the Russian Academy of Sciences, Acad. Lavrentiev Ave., 3, Novosibirsk 630090, Russia
[d] Novosibirsk State University, 2 Pirogova Str., Novosibirsk 630090, Russia
[e] Institute of Physics SB RAS, Federal Research Center "Krasnoyarsk Science Center SB RAS", Akademgorodok, 50-38, Krasnoyarsk 660036, Russia

ARTICLE INFO

Keywords:
Vinylidene complexes
Rhenium
Platinum
NMR
X-ray diffraction
Redox properties

ABSTRACT

Reactions of $Cp(CO)_2Re{=}C{=}CHPh$ with $Pt[P(OR)_3]_4$ (R = Pr^i, Et, Ph) gave binuclear μ-vinylidene complexes $Cp(CO)_2RePt(\mu\text{-}C{=}CHPh)[P(OR)_3]_2$. Treatment of the previously synthesized $Cp(CO)_2Re(\mu\text{-}C{=}CHPh)Pt(PPh_3)_2$ with triisopropylphosphite or triethylphosphite resulted in a stepwise substitution of PPh_3 ligands, leading to the disubstituted $Cp(CO)_2RePt(\mu\text{-}C{=}CHPh)[P(OR)_3]_2$ and monosubstituted $Cp(CO)_2RePt(\mu\text{-}C{=}CHPh)[P(OR)_3](PPh_3)$ (R = Pr^i or Et) species, while no triphenylphosphine ligand substitution in the reaction with $P(OPh)_3$ occurs at all. The monosubstituted $Cp(CO)_2RePt(\mu\text{-}C{=}CHPh)[P(OR)_3](PPh_3)$ (R = Pr^i, Et, Ph) species were also obtained by reacting $Cp(CO)_2Re{=}C{=}CHPh$ with mixed-ligand complexes $Pt(PPh_3)_3L$ (L = $P(OPr^i)_3$, $P(OEt)_3$, $P(OPh)_3$). Reactions of $Cp(CO)_2RePt(\mu\text{-}C{=}CHPh)LL'$ (L = L′ = $P(OPr^i)_3$, $P(OEt)_3$, $P(OPh)_3$; L = $P(OPr^i)_3$, $P(OEt)_3$, $P(OPh)_3$, L′ = PPh_3) with $Co_2(CO)_9$ yield tricarbonyl vinylidene species $Cp(CO)_2RePt(\mu\text{-}C{=}CHPh)[P(OR)_3](CO)$ (R = Pr^i, Et, Ph). The obtained compounds were characterized by IR and ^1H, ^{13}C, ^{31}P NMR spectroscopy. The molecular structures of $Cp(CO)_2RePt(\mu\text{-}C{=}CHPh)[P(OPr^i)_3]_2$, $Cp(CO)_2RePt(\mu\text{-}C{=}CHPh)[P(OPr^i)_3](PPh_3)$ and $Cp(CO)_2RePt(\mu\text{-}C{=}CHPh)[P(OPr^i)_3](CO)$ were determined by X-ray diffraction study. The redox properties of the new complexes and their reactions of chemical oxidation were studied.

1. Introduction

The chemistry of heteropolynuclear metal clusters and complexes containing π-conjugated polycarbon ligands have received the attention of researchers in view of possible applications of some of such compounds in functional material development, molecular devices design, biochemistry, and catalysis [1–3]. For instance, the cooperativity and synergistic effects of these heterometallic compounds arisen from the simultaneous or consecutive action of their metal centers on substrates make them attractive compounds for molecular activation that mononuclear complexes are not able to achieve [4–9]. The heteropolynuclear compounds can be used as single-source precursors for heterogeneous catalysts that offer the potential of fine-tuning their intermetallic ratio and retaining it in the resulting heterometallic particles [4,10]. Thus, understanding interactions between metals, metals and their ligand environment, and between ligands in the hetropolynuclear complexes are essential not only to their chemistry, but also to the possible application of them [11–13]. A variety of synthetic approaches to the heterometallic compounds are known [1,14].

The heterometallic vinylidene bridged complexes and clusters are one type of such compounds. A vast majority of those has been obtained in studies on activation and transformations of alkynes and alkenes on heteropolynuclear complexes [15–24]. However, the most reliable and predictable methods for their synthesis are metal fragment condensation reactions and ligand substitution reactions. A wide variety of heterometallic vinylidene complexes [25–30] and clusters [25,31]

* Corresponding author.
E-mail addresses: vvv@sany-ok.ru, vvv@icct.ru (V.V. Verpekin).

https://doi.org/10.1016/j.ica.2020.119463
Received 4 October 2019; Received in revised form 15 January 2020; Accepted 20 January 2020
Available online 23 January 2020

containing MM′, MM′$_2$ and MM′M″ cores were prepared by reaction of mononuclear vinylidene complexes of the type $L_nM{=}C{=}CR_2$ with unsaturated metal-containing fragments. Whereas, the second method were only applied to the synthesis of a series of binuclear μ-vinylidene MnM (M = Pt, Pd) complexes [32–35]. In our previous works we reported a preparation of the binuclear $Cp(CO)_2ReM(\mu\text{-}C{=}CHPh)(PPh_3)_2$ μ-vinylidene complexes through the reaction of the rhenium vinylidene $Cp(CO)_2Re{=}C{=}CHPh$ and $M(PPh_3)_4$ (M = Pt, Pd) [36]. The possibility of substitution of both PPh_3 groups by chelate diphosphine ligands or one PPh_3 group by carbon monoxide in these binuclear complexes was demonstrated [37–39].

In this article, we explored an applicability of several synthetic approaches to binuclear μ-vinylidene RePt complexes with terminal phosphite ligands at the Pt atom. We also tried to evaluate an influence of ligand environment of the Pt atom in the synthesized compounds on the spectroscopic, structural, and electrochemical properties. A behavior of the new and previously synthesized RePt μ-vinylidene complexes in oxidation reactions was studied.

2. Results and discussion

2.1. Synthesis of the binuclear $Cp(CO)_2RePt(\mu\text{-}C{=}CHPh)LL'$ complexes

Binuclear RePt complexes of the type $Cp(CO)_2RePt(\mu\text{-}C{=}CHPh)L_2$ [L = $P(OPr^i)_3$ (**1a**), $P(OEt)_3$ (**2a**), $P(OPh)_3$ (**3a**)] were isolated from reactions of $Cp(CO)_2Re{=}C{=}CHPh$ with $Pt[P(OR)_3]_4$ (R = Pr^i, Et, Ph) in 63%, 61%, and 91% yields, respectively. The moderate yields of the complexes **1a** and **2a** were caused by side reactions of the starting rhenium vinylidene with free phosphites, produced by dissociation of $Pt[P(OR)_3]_4$ in the reaction mixture, that initially resulted in extremely sensitive to water zwitter-ionic byproducts $Cp(CO)_2Re\text{-}C(^+P(OR)_3){=}CHPh$ that then hydrolyzed upon a chromatography of the reaction mixtures to give the corresponding η^2-phosphorylalkene complexes $Cp(CO)_2Re\{\eta^2\text{-}E\text{-}HC[P(O)(OR)_2]{=}C(H)Ph\}$ (R = Pr^i, Et) in 10 and 16% yields (Scheme 1) [40]. However, in case of $Pt[P(OPh)_3]_4$ the formation of the byproduct wasn't observed because of low nucleophilicity of $P(OPh)_3$ and low rate of its reaction with the rhenium vinylidene [40].

In order to avoid the formation of the zwitter-ionic byproducts, reactions of PPh_3 ligand substitution in $Cp(CO)_2RePt(\mu\text{-}C{=}CHPh)(PPh_3)_2$ (**4**) by the phosphites were investigated. The treatment of **4** with $P(OPr^i)_3$ and $P(OEt)_3$ in 1:2 M ratios resulted in two products: disubstituted $Cp(CO)_2RePt(\mu\text{-}C{=}CHPh)L_2$ [L = $P(OPr^i)_3$ (**1a**), $P(OEt)_3$ (**2a**)] and monosubsituted $Cp(CO)_2RePt(\mu\text{-}C{=}CHPh)(PPh_3)L$ [L = $P(OPr^i)_3$ (**1b**), $P(OEt)_3$ (**2b**)] complexes in about 70% and 30% yields, respectively (Scheme 1). When the reactions of **4** with phosphites were performed with at least reactant ratio 1:4, the amount of the disubstituted complexes **1a** and **2a** were dramatically increased up to 99%. Thus, the formation of the monosubstituted species **1b** and **2b** in these reactions evidenced that substitution of PPh_3 ligands in **4** by the phosphites should occur stepwise to give the monosubstituted species ***b*** at the beginning of the described reactions. Indeed, the triphenylphosphine ligand in complexes **1b** and **2b** can be easily substituted by phosphites, resulting in formation of the disubstituted species **1a** and **2a** in high yields. The reaction of **4** with one equivalent of the triisopropyl or triethylphosphite gave a mixture of products with the major constituent being the monosubstituted complex **1b** or **2b**, but traces of initial **4** and disubstituted species **1a** or **2a** were still presented in the reaction mixture (Scheme 2, *reaction a*).

Our attempts to obtain complex **3a** or at least monosubstituted complex $Cp(CO)_2RePt(\mu\text{-}C{=}CHPh)(PPh_3)[P(OPh)_3]$ (**3b**) by using the PPh_3 ligand substitution approach didn't give any results, a reaction between **4** and $P(OPh)_3$ didn't proceed at all. However, the monosubstituted complex $Cp(CO)_2RePt(\mu\text{-}C{=}CHPh)(PPh_3)[P(OPh)_3]$ (**3b**) was eventually obtained by the reaction of $Cp(CO)_2Re{=}C{=}CHPh$ with a mononuclear mixed-ligand complex $Pt(PPh_3)_3[P(OPh)_3]$ [41], which was generated by addition of one equivalent $P(OPh)_3$ to benzene solution of $Pt(PPh_3)_4$ (Scheme 2, *reaction d*). Further substitution of PPh_3 ligand in **3b** by $P(OPh)_3$ occurs easily to give $Cp(CO)_2RePt(\mu\text{-}C{=}CHPh)[P(OPh)_3]_2$ (**3a**). On the other hand, our efforts to obtain complexes **1b** and **2b** by this approach were unsuccessful, their yields didn't exceed 40%, and the main product was complex **4** in both cases.

The disubstituted complexes of type ***a*** upon treatment with excess of PPh_3 are able to transform into **1b-3b** (Scheme 2, *reaction b*), but these reactions are slow in contrast to the reactions of **4** with $P(OPr^i)_3$ or $P(OEt)_3$. So, reactions of **1a–3a** with five equivalents PPh_3 performed over 12 h at room temperature gave the monosubstituted species only in about 50% yields, followed heating of these mixtures at 60 °C within the same period of time led to complete conversion of the disubstituted complexes to the monosubstituted **1b-3b**. Although, the unwanted formation of complex **4** in such condition took place, but its yields didn't exceed 10%.

Earlier [33], a disproportionation of the $Cp(CO)_2MnPt(\mu\text{-}C{=}CHPh)(PPh_3)[P(OPr^i)_3]$ in solution at room temperature were found to result in the bis(phosphine) $Cp(CO)_2MnPt(\mu\text{-}C{=}CHPh)(PPh_3)_2$ and the bis(triisopropylphosphite) $Cp(CO)_2MnPt(\mu\text{-}C{=}CHPh)[P(OPr^i)_3]_2$ complexes, which also could react with each other to give the initial monosubstituted product. We examined a possibility of such equilibrium in the solutions of complex **4** and $Cp(CO)_2RePt(\mu\text{-}C{=}CHPh)[P(OR)_3]_2$ [R = Pr^i (**1a**), Et (**2a**)]. The 24 h NMR monitoring of stoichiometric amounts of bis(phosphite) complex (**1a** or **2a**) and **4** showed an absence of such process in solutions at room temperature. However,

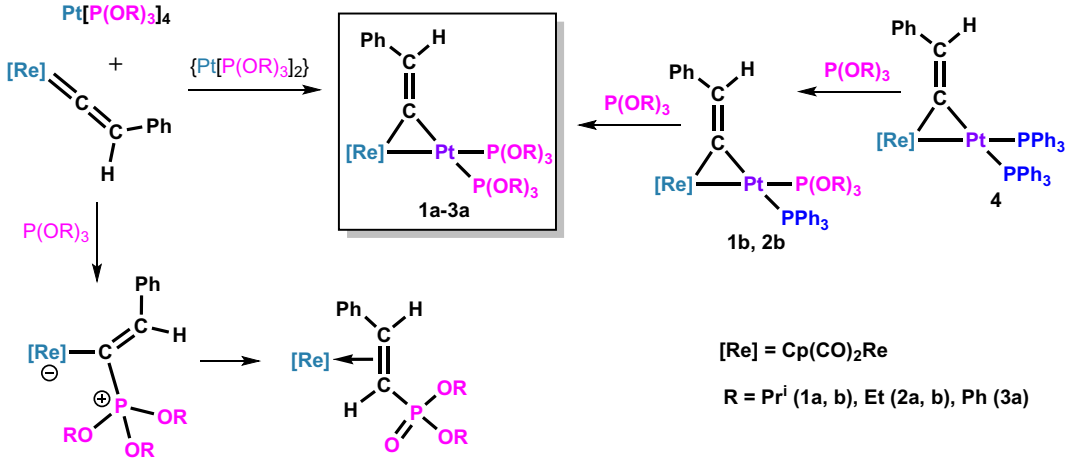

Scheme 1.

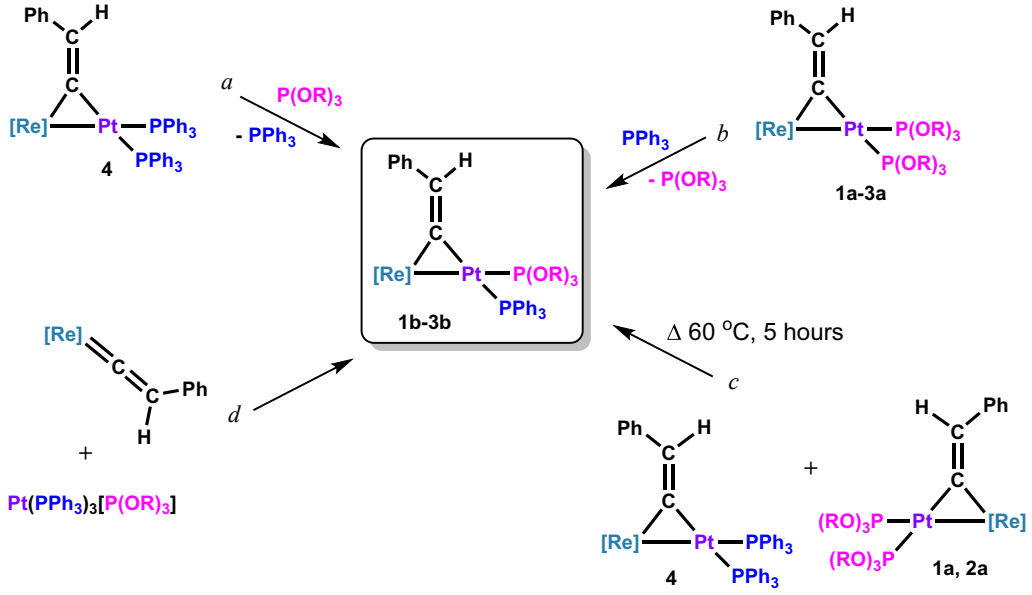

reaction	Yield* / Isolated (%)		
	1b	**2b**	**3b**
a	75/65	76/67	no reaction
b	50 / 37	48 / 36	60 / -
c	82 / 70	76 / 70	-
d	38 / -	40 / -	91 / 88

* According to NMR ^{31}P data

Scheme 2.

after heating of these reaction mixtures, the signals of $Cp(CO)_2RePt(\mu$-C═CHPh)(PPh_3)[L] (L = $P(OPr^i)_3$ (**1b**), $P(OEt)_3$ (**2b**)) were detected in ^{31}P NMR spectra. Eventually, the highest yields in 82% of **1b** and 76% of **2b** were achieved by performing the reactions of **4** and $Cp(CO)_2RePt(\mu$-C═CHPh)$[P(OR)_3]_2$ [R = Pr^i (**1a**), Et (**2a**)] at 60 °C for 5 h (Scheme 2, *reaction c*).

We also investigated possibility of substitution of phosphorous-donor ligands at the platinum atom in the obtained binuclear vinylidenes by carbon monoxide. Previously, RePt and MnPt complexes of the type $[Cp(CO)_2MPt(\mu$-C═CHPh)$(PPh_3)(CO)]$ (M = Re (**5**), Mn) were prepared by the reaction of $[Cp(CO)_2MPt(\mu$-C═CHPh)$(PPh_3)_2]$ (M = Re (**4**), Mn) and $Co_2(CO)_8$ [33,39]. Following this strategy, we prepared a series of RePt μ-vinylidene complexes with the platinum-bound CO ligands $Cp(CO)_2RePt(\mu$-C═CHPh)(CO)L [L = $P(OPr^i)_3$ (**1c**), $P(OEt)_3$ (**2c**), $P(OPh)_3$ (**3c**)] in high yields (Scheme 3). It should be noted that all performed reactions led to a selective substitution of the Pt-bound phosphite or phosphine ligand being *trans to* the bridging vinylidene ligand. So in complexes **1a–3a** one of the Pt-bound $P(OR)_3$ ligand were replaced by CO, whereas in complexes of type ***b*** replacement of phosphine ligand at the Pt atom occurred. Such reactivity of the complexes reflects the high *trans*-influence of the bridging vinylidene ligand.

The chemistry of the obtained tricarbonyl complexes is identical to previously synthesized complex **5** [39]. For example, the Pt-bound CO ligand in **1c–3c** can be readily substituted upon addition of different nucleophiles like triphenylphosphine to give complexes $Cp(CO)_2RePt(\mu$-C═CHPh)(PPh_3)L [L = $P(OPr^i)_3$ (**1b**), $P(OEt)_3$ (**2b**), $P(OPh)_3$ (**3b**)], or phosphites to regenerate initial complexes **1a**, **2a**, and **3a** in high yields. In case of diphosphines displacement of both CO and phosphorus-donor ligands occurs to yield the known RePt complexes with chelate diphosphine ligands at the Pt atom [37].

2.2. NMR and IR study of $Cp(CO)_2RePt(\mu$-C═CHPh)LL′ complexes

The ^{1}H, ^{13}C, ^{31}P NMR and the IR data for the complexes **1a–3c** were obtained (Tables 1, 2). The NMR signals of complexes **1a**, **1b**, and **4** were assigned on the basis of ^{1}H, ^{13}C{^{1}H} and ^{1}H, ^{31}P{^{1}H} correlations. The structure of the complexes can be deduced from the combined NMR

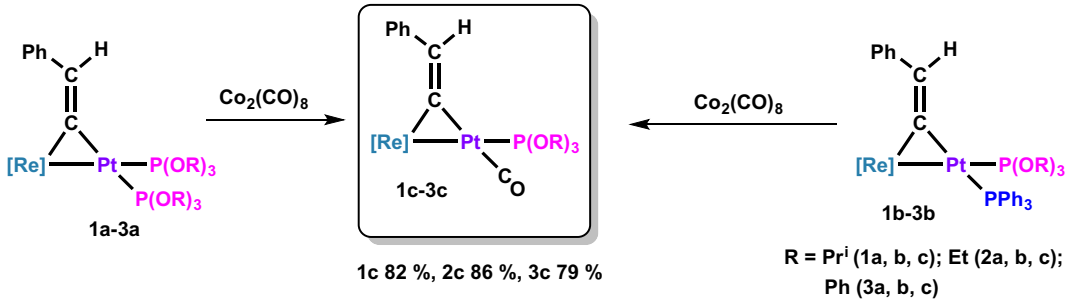

Scheme 3.

Table 1
NMR (δ, ppm [J, Hz]) spectroscopic data for the $Cp(CO)_2RePt(\mu\text{-}C{=}CHPh)LL'$ (L = L′ = $P(OPr^i)_3$ (**1a**), $P(OEt)_3$ (**2a**), $P(OPh)_3$ (**3a**); L′ = PPh_3, L = $P(OPr^i)_3$ (**1b**), $P(OEt)_3$ (**2b**), $P(OPh)_3$ (**3b**); L′ = CO, L = $P(OPr^i)_3$ (**1c**), $P(OEt)_3$ (**2c**), $P(OPh)_3$ (**3c**)).

	NMR							
	^{13}C				^1H		^{31}P	
	$\mu\text{-}C^1{=}C^2HPh$		C_5H_5	CO	$=C^2HPh$	C_5H_5	P^1	P^2
	C^1	C^2						
1a [a]	228.0 dd J_{PtC} = 790.8 $^2J_{PC}$ = 92.8 $^2J_{PC}$ = 4.8	138.4 dd $^2J_{PtC}$ = 108.2 $^3J_{PC}$ = 6.1 $^3J_{PC}$ = 2.8	85.5 s	202.0 s	8.42 ddd $^4J_{PH}$ = 14.5 $^4J_{PH}$ = 22.4 $^3J_{PtH}$ = 14.8	5.34 s	138.0 dd, $^2J_{PP}$ = 6, J_{PtP} = 6811	146.1 dd, $^2J_{PP}$ = 6, J_{PtP} = 3958
2a [b]	228.8 ddd J_{PtC} = 791.8 $^2J_{PC}$ = 93.3 $^2J_{PC}$ = 5.2	138.5 ddd $^3J_{PC}$ = 5.2 $^3J_{PC}$ = 2.6 $^2J_{PtC}$ = 109.2	85.1 s	202.1 s	8.90 ddd $^4J_{PH}$ = 23.4 $^4J_{PH}$ = 15.3 $^3J_{PtH}$ = 15.8	5.08 s	135.5 dd $^2J_{PP}$ = 4 J_{PtP} = 6753	148.4 dd, $^2J_{PP}$ = 4, J_{PtP} = 3924
3a [b]	229.5 dd J_{PtC} = 781.7 $^2J_{PC}$ = 92.3	140.6 dd $^3J_{PC}$ = 4.2 $^2J_{PtC}$ = 102.7	85.9 s [b]	–[c]	8.32 ddd [b] $^4J_{PH}$ = 24.8 $^4J_{PH}$ = 15.7 $^3J_{PtH}$ = 18.8	4.83 s	118.1 dd, $^2J_{PP}$ = 14, J_{PtP} = 6919	136.1 dd, $^2J_{PP}$ = 14, J_{PtP} = 4179
1b [a]	228.0 dd $^2J_{PC}$ = 63.8 $^2J_{PC}$ = 6.6	137.0 dd $^2J_{PtC}$ = 115.2 $^3J_{PC}$ = 3.3 $^3J_{PC}$ = 3.3	85.1 s	202.8 s, br	8.49 dd $^4J_{PH}$ = 15.1, $^4J_{PH}$ = 15.1, $^3J_{PtH}$ = 8.2	4.86 s	130.1 d, J_{PtP} = 7235	28.4 d, J_{PtP} = 2329
2b [b]	227.6 dd $^2J_{PC}$ = 62.1 $^2J_{PC}$ = 6.2	136.2 ddd $^2J_{PtC}$ = 112.4 $^3J_{PC} \approx {}^3J_{PC}$ = 2.7	85.0 s	202.5 s	8.91 ddd $^3J_{PtH}$ = 7.3 $^4J_{PH} \approx {}^4J_{PH}$ = 15.3	4.63 s	133.3 d, J_{PtP} = 7193	29.1 d, J_{PtP} = 2340
3b [b]	228.8 dd $^2J_{PC}$ = 57.9 $^2J_{PC}$ = 4.9	138.76 d $^2J_{PtC}$ = 100.9	85.1 s	201.2 br. s	9.04 ddd $^3J_{PtH}$ = 14.4, $^4J_{PH} \approx {}^4J_{PH}$ = 15.9	4.84 s	122.3 d, J_{PtP} = 7525	28.5 d, J_{PtP} = 2444
1c [b]	227.0 dd J_{PtC} = 841.0 $^2J_{PC}$ = 3.8	142.2 dd $^2J_{PtC}$ = 112.7 $^3J_{PC}$ = 4.5	86.0 s	195.4 dd J_{PtC} = 1217 $^2J_{PC}$ = 1.7, (Pt-CO) 202.9 br. s (Re-CO)	8.92 dd $^4J_{PH}$ = 14.4, $^3J_{PtH}$ = 19.5	4.78 s	122.1 d, J_{PtP} = 6442	–
2c [b]	227.4 d, $^2J_{PC}$ = 3.5	142.3 dd, $^2J_{PtC}$ = 110.6 $^3J_{PC}$ = 4.9	85.7 s	196.4 d, $^2J_{PC}$ = 1.7, (Pt-CO) –[c]	8.88 dd $^4J_{PH}$ = 14.9, $^3J_{PtH}$ = 19.4	4.78 s	124.5 d, J_{PtP} = 6441	–
3c [b]	227.7dd J_{PtC} = 867.0 $^2J_{PC}$ = 3.8	142.8 dd $^2J_{PtC}$ = 104.4 $^3J_{PC}$ = 4.5	85.9 s	193.2 dd J_{PtC} = 1231 $^2J_{PC}$ = 2.4 (Pt-CO) 200.8 br. s. (Re-CO)	8.84 dd $^4J_{PH}$ = 14.5 $^3J_{PtH}$ = 25.7	5.11 s	115.0 d, J_{PtP} = 6765	–
4	232.2 d J_{PtC} = 821.6 $^2J_{PC}$ = 65.3	138.3 dd $^2J_{PtC}$ = 96.2 $^3J_{PC}$ = 4.0	85.7 s	204.5 s, br	–[d]	4.81 s	39.3 dd, $^2J_{PP}$ = 22 J_{PtP} = 4609	28.1 dd, $^2J_{PP}$ = 22 J_{PtP} = 2607
5	229.7 s J_{PtC} = 855.0	143.2 dd $^2J_{PtC}$ = 104.0 $^3J_{PC}$ = 5.5	86.2 s	196.2 s J_{PtC} = 1280 202.9 s, br	7.41 s	5.37 s	31.21 d, J_{PtP} = 4069	–

NMR spectra were measured.
[a] $InCD_2Cl_2$ solution.
[b] In $CDCl_3$ solution, and the rest in C_6D_6 solution.
[c] The CO signals were broadened so much that they were not detected.
[d] The $= C^2\boldsymbol{H}Ph$ signal is masked by the resonances of phenyl groups.

and IR data, which are similar to those of previously described μ-vinylidene complexes with RePt and MnPt cores [32,33,36,37].

The ^1H NMR spectra of the complexes show a characteristic vinylidene hydrogen $=C^2H$ between 8.3 and 9.1 ppm [25,30] as a doublet of doublets (**1c–3c**) or a doublet of doublets of doublets (**1a–3a, 1b–3b**). The ^{13}C chemical shifts of the α- and β-vinylidene carbons of **1a–3c** resonate as a doublet of doublets in the regions δ 228–300 and δ 136–143 ppm, respectively. It should be noted that in the ^{13}C NMR spectra the signals of $\mu\text{-}C_\alpha$-vinylidene atom of synthesized complexes are upfield shifted by 32 ppm in comparison to those of corresponding MnPt complexes [33].

The ^{13}C NMR spectra of **1a–3c** contain broad resonances or sharp singlets (**1a**, **1b**, and **2a**) in the narrow interval 200–203 ppm that were assigned to the two Re-bound CO ligands. The coalescence of the two CO resonances can be explained by a site exchange of two carbonyl groups of the $[Cp(CO)_2Re]$ fragment and has been observed earlier [37–39,42–44]. The presence of the platinum coordinated carbonyl group in the ^{13}C NMR spectra of **1c–3c** is indicated by signals around 199 ppm with characteristic J_{PtC} coupling about 1224 Hz.

The ^{31}P NMR spectra of type ***a*** and ***b*** complexes show two signals corresponding to two non-equivalent phosphorus nuclei (Table 1). ^{31}P NMR signal assignment was made on the basis of previously published works [37,39,45]. The signal with a larger coupling constant is assigned to the ligand *trans to* the rhenium and the signals with a smaller J_{PtP}

Table 2
IR data for the $Cp(CO)_2RePt(\mu\text{-}C{=}CHPh)LL'$.

	ν(CO), cm^{-1}	$\Delta\nu$(CO)
$Cp(CO)_2RePt(\mu\text{-}C{=}CHPh)[P(OPr^i)_3]_2$ (**1a**)	1943 s, 1873 s	70
$Cp(CO)_2RePt(\mu\text{-}C{=}CHPh)[P(OEt)_3]_2$ (**2a**)	1940 s, 1870 s	70
$Cp(CO)_2RePt(\mu\text{-}C{=}CHPh)[P(OPh)_3]_2$ (**3a**)	1952 s, 1881 s	71
$Cp(CO)_2RePt(\mu\text{-}C{=}CHPh)[P(OPr^i)_3](PPh_3)$ (**1b**)	1935 s, 1859 s	76
$Cp(CO)_2RePt(\mu\text{-}C{=}CHPh)[P(OEt)_3](PPh_3)$ (**2b**)	1936 s, 1860 s	76
$Cp(CO)_2RePt(\mu\text{-}C{=}CHPh)[P(OPh)_3](PPh_3)$ (**3b**)	1945 s, 1873 s	72
$Cp(CO)_2RePt(\mu\text{-}C{=}CHPh)[P(OPr^i)_3](CO)$ (**1c**)	2030 s (Pt-CO), 1940 s, 1878 s	62
$Cp(CO)_2RePt(\mu\text{-}C{=}CHPh)[P(OEt)_3](CO)$ (**2c**)	2041 s (Pt-CO), 1939 s, 1876 m.	63
$Cp(CO)_2RePt(\mu\text{-}C{=}CHPh)[P(OPh)_3](CO)$ (**3c**)	2046 s (Pt-CO),1953 s, 1889 s	63
$Cp(CO)_2RePt(\mu\text{-}C{=}CHPh)(PPh_3)_2$ (**4**)	1933 s, 1858 m,br	75
$Cp(CO)_2RePt(\mu\text{-}C{=}CHPh)(PPh_3)(CO)$ (**5**)	2030 s (Pt-CO), 1941 s, 1878 m	63

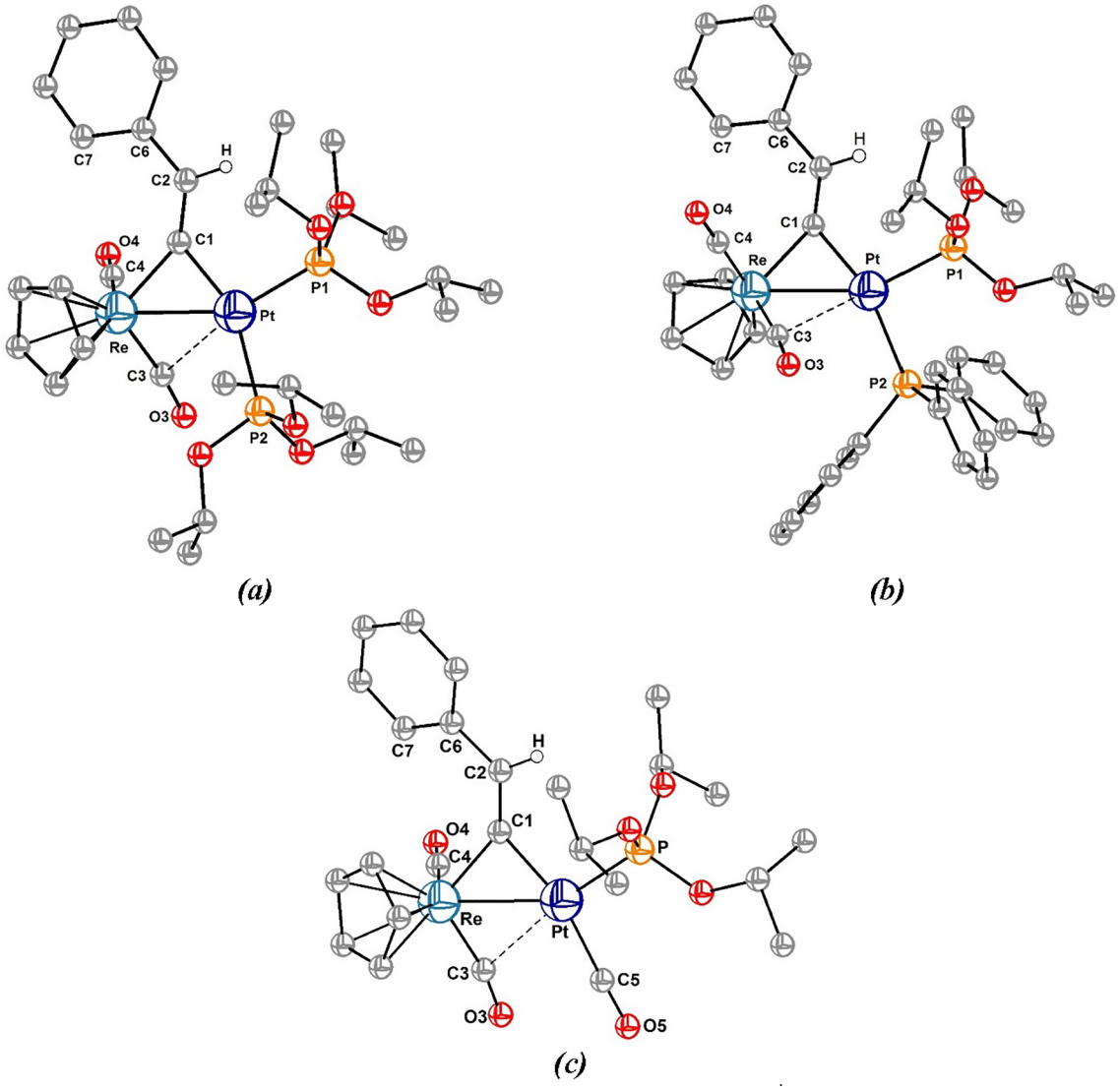

Fig. 1. Molecular structures of $Cp(CO)_2RePt(\mu\text{-}C{=}CHPh)[P(OPr^i)_3]_2$ (**1a**) – ***(a)***; $Cp(CO)_2RePt(\mu\text{-}C{=}CHPh)[P(OPr^i)_3](PPh_3)$ (**1b**) – ***(b)***; $Cp(CO)_2RePt(\mu\text{-}C{=}CHPh)[P(OPr^i)_3](CO)$ (**1c**) – ***(c)***. All hydrogen atoms in **1a–c** except that of the phenylvinylidene ligand are omitted for clarity.

coupling is assigned to the ligand *trans to* the μ-C═CHPh. Thus, the *trans* position of PPh_3 ligand to vinylidene in **1b-3b** is indicated by high field doublet with average J_{PtP} coupling of 2370 Hz at around δ 28.5 ppm in the ^{31}P NMR spectrum. In the case of complexes **1c–3c** containing one phosphite and one carbonyl ligands at the platinum atom the magnitude of the J_{PtP} coupling indicates the *trans* position of P $(OR)_3$ to the rhenium fragment.

The ^{31}P NMR spectra of the type ***a*** complexes showed the signals of both phosphite ligands as doublets with resolved $^2J_{PP}$ coupling constants, whereas the signals of phosphite and phosphine ligands in the spectra of the type ***b*** complexes appeared as singlets. Our attempts to obtain the resolved spectra by changing solvent or temperature were

unsuccessful. Therefore, these observations should be explained by the assumption that the presence in the ***b*** complexes of two electronically different phosphorous-donor ligands leads to reducing of magnetic moment interaction of their nuclei. As a result, their $^2J_{PP}$ values do not exceed the width at half height of peaks (ca. 2 Hz) and so resonances of ligands in ^{31}P NMR spectra of **1-3b** appear as singlets.

In general, the obtained NMR spectroscopic data of the complexes showed that there is no significant influence of the ligand environment of the platinum atom on the bridging phenylvinylidene moiety. Although, it should be noted that the signals of $=C^2$ nucleus in ^{13}C NMR spectra of complexes of the type ***c*** are slightly downfield shifted by 2–4 ppm compared with the signals of the same nucleus of **1a–3b.** A comparison of NMR spectra data of **1a–3c** and previously studied RePt complexes with chelate diphosphine ligands [37,39,46] demonstrates that the resonances of μ-C^1 nucleus in ^{13}C NMR spectra of the new phosphite-containing complexes are upfield shifted by 4–5 ppm.

The IR spectra of **1a–3b** in CH_2Cl_2 solutions shows two ν(CO) bands that are attributed to the carbonyl groups at the Re atom (Table 2). The position of the ν(CO) bands indicates that CO ligands are non-equivalent. The first high-frequency ν(CO_t) band is terminal. The low-frequency ν(CO_{sb}) band is semibridging due to an influence of the adjacent Pt atom. The high frequency shift of both ν(CO) bands in the IR specta of **1a–3b** is observed as compared to that of the previously synthesized RePt complexes with the chelate diphosphine ligands [37]. This observation indicates that a Pt → CO_{sb} interaction in the new complexes of type ***a*** and ***b*** is weaker than in the previously synthesized RePt complexes [37,46]. The substitution of one of the phosphorous-donor ligands by carbonyl group leads to reduction of Pt → CO_{sb} interaction in the type ***c*** complexes in contrast to **1a–3b**. A difference between the stretching vibration bands of two carbonyl groups Δν(CO) = ν(CO_t) − ν(CO_{sb}) [32] clearly demonstrates that the degree of semibridging Pt → CO_{sb} interaction in the complexes decreased in the range **1b**-**3b** → **1a–3a** → **1c–3c** (Table 2).

*2.3. Crystal structures of Cp(CO)$_2$RePt(μ-C═CHPh)[P(OPr^i)$_3$]$_2$ (**1a**), Cp(CO)$_2$RePt(μ-C═CHPh)[P(OPr^i)$_3$](PPh$_3$) (**1b**), Cp(CO)$_2$RePt(μ-C═CHPh)[P(OPr^i)$_3$](CO) (**1c**)*

The molecular structures of Cp(CO)$_2$RePt(μ-C═CHPh)[P(OPr^i)$_3$]$_2$ (**1a**), Cp(CO)$_2$RePt(μ-C═CHPh)[P(OPr^i)$_3$](PPh$_3$) (**1b**), and Cp(CO)$_2$RePt(μ-C═CHPh)[P(OPr^i)$_3$](CO) (**1c**) were solved on the base of X-ray diffractometry. Suitable crystals of **1a–c** were grown from hexane and hexane:diethyl ether mixture. The views of the structures are shown in Fig. 1. Crystal data and refinement parameters are shown in Table 3. Selected bond distances and angles of the complexes are given in Table 4.

The Re- and Pt-containing moieties of the complexes are bridged by the μ-vinylidene ligand to give a cycle RePtC1. The Re-C1, Pt-C1, C1═C2 bond distances and Re-C1-Pt, C1-Pt-Re, Pt-Re-C1 bond angles of **1a–c** are close to each other and similar to that of the known μ-vinylidene RePt complexes [37,39]. Values of a dihedral angle between the ReC1Pt and C1C2C6 planes of the complexes **1a** (3.4(5)°), **1b** (1.9(3)°) and **1c** (7.6(1)°) clearly indicate that the μ-C═CHPh ligand is located in a plane of RePtC1 carbodimetallacycle. Values of a torsion angle C7-C6-C2-C1 of the complexes are given in Table 4.

The Re-Pt distances of **1a–c** are shorter than the sum of the covalent radii of the Re and Pt atoms [47] and, thus, should be considered as bonding. A comparison of the RePt bond lengths of **1a–c** with those of the previously structurally characterized complexes **4** and **5** indicates that the substitution of PPh_3 by less σ-donor P(OPr^i)$_3$ ligand lead to decrease in these parameters. For instance, the distance between the Re and the Pt atoms is consistently reduced on going from 2.7360(3) (**4**) to 2.7281(5) (**1b**) and to 2.7154(5) Å (**1a**). However, the complex **1c** stands out from this trend that is probably a consequence of presence of weak σ-donor P(OPr^i)$_3$ and strong π-acceptor CO ligands on the Pt fragment.

Complex **1a** crystallized with two crystallographically independent molecules, which significantly differ in orientation of Pr^i-substituents and slightly in geometric parameters (Table 4, Fig.11 of supplementary data). In complexes **1b** and **1c** a disordering of OPr^i-groups of P^1(OPr^i)$_3$ ligand is observed. Two CH_3-groups of one Pr^i-substituent are occupying two equivalent positions in **1c**. Whereas in complex **1b** the two OPr^i-groups of P(OPr^i)$_3$ ligand *trans* to rhenium are occupying two positions with ca. 40% and 60% probability, respectively. In addition, **1b** crystallized with a molecule of hexane with 40% occupation. Moreover, such location of the solvent is not by a chance as one of the hexanes atom is close to position of terminal carbon (corresponding C…C distance is 2.50 Å) of the disordered Pr^i-group with 60% occupation. Thus, the molecule of the solvent in the complex **1b** sterically affects the positions of OPr^i-grops of the ligand (Fig. 12 of supplementary data). Since those atoms are highly disordered, all C—C distances were constrained to 1.54 Å with DFIX instructions and angle C4H-C5H-C6H was constrained with DANG 2.4 instruction. Thermal motion of hexane atoms was treated as isotropical.

The geometry of ligand environment around the platinum atom in **1a–c** is distorted square planar. The average P1-Pt-P2 bond angle of two independent molecules in **1a** is 102.19(7)° and close to the value of 102.99(4)° in complex Cp(CO)$_2$RePt(μ-C═CHPh)(PPh$_3$)$_2$ (**4**), whereas the same angle in **1b** is smaller by *ca.* 7° (Table 4). In the case of complex Cp(CO)$_2$RePt(μ-C═CHPh)[P(OPr^i)$_3$](CO) (**1c**) the P1-Pt-C5 bond angle (97.2(4)°) is also reduced in comparison with that of 99.7(4)° in Cp(CO)$_2$RePt(μ-C═CHPh)(PPh$_3$)(CO) (**5**). Herewith, the values C1PtRe bond angles in **1a–c** are close to each other, and similar to those that were found in the known RePt complexes [37,39].

As mentioned above, the IR spectra of complexes **1a–c** indicated the presence of considerably weak semibridging interaction between the platinum atom and the C3O3 carbonyl group of the Re fragment, which decreased in the range **1b** → **1a** → **1c**. Indeed, the obtained structural data confirmed this assumption, the Pt-C3 bond distances in **1b** and **1c** (2.709(4) and 2.712(9) Å respectively) reflect the presence of bonding interaction between the adjacent platinum atom and C3O3 group. Although, a large value of the Pt-C3 distances in **1a** (2.772(10) and 2.837(10) Å) might be interpreted as indicating the lack of the semibridging interaction, however a deviation of the Re-C3-O3 bond angle (168.416(3)°) from linearity clearly demonstrate the presence of such interaction. Note, the short Pt-C3 distance in **1c** should be explained by much smaller steric effect of adjacent C5O5 group in comparison with P(OPr^i)$_3$ or PPh_3 ligands.

2.4. Electrochemical study

The redox properties of the binuclear μ-vinylidene complexes **1a–3c**, **4**, and **5** were studied in acetonitrile solutions using dc polarography at a dropping mercury electrode (DME), cyclic voltammetry (CV) at platinum or glassy carbon (GC) electrodes,[1] and controlled potential electrolysis (CPE) at a Pt-electrode. The electrochemical characteristics of these complexes and the mononuclear rhenium vinylidene are given in Table 5. The cyclic voltammograms of complexes **2a–2c** and Cp(CO)$_2$Re═C═CHPh at the GC-electrode are given in Fig. 2.

A comparison of the obtained electrochemical data clearly showed that first oxidation and reduction potentials of the binuclear RePt complexes (**1a–3c, 4**, and **5**) depend on the nature of ligands at the Pt atom. So, an anodic shift in $E_{1/2}$ values is observed on moving from P(OPr^i)$_3$- to P(OEt)$_3$- and to P(OPh)$_3$-containing complexes that is

[1] The application of different working electrodes offers an opportunity to study the oxidation and reduction properties of compounds in the wide range of accessible potentials. The measurement region of potentials in acetonitrile (vs. Ag/0.1 M $AgNO_3$ in MeCN) is from 0.30 to −3.20 V at DME, from 2.0 to −2.2 V, and from 2.0 to −2.6 V at the Pt and GC electrodes, respectively.

Table 3
Crystal data and X-ray experimental details for complexes **1a–c**.

Complex	1a	1b	1c
Empirical formula	$C_{33}H_{53}O_8P_2RePt$	$C_{44.4}H_{52.6}O_5P_2PtRe$	$C_{25}H_{32}O_6PRePt$
Formula weight	1020.98	1109.49	833.71
Temperature/K	150.0	150.0	296
Crystal system	triclinic	monoclinic	triclinic
Space group	*P*-1	$P2_1/n$	*P*-1
a/Å	11.7690(6)	14.8319(5)	8.7502(4)
b/Å	15.8882(8)	20.7754(6)	11.8179(7)
c/Å	21.4707(12)	15.1651(5)	14.7854(8)
α/°	92.347(2)	90.00	105.6448(12)
β/°	99.2166(18)	100.2408(12)	101.4502(10)
γ/°	105.0981(17)	90.00	91.3875(13)
Volume/Å^3	3811.7(3)	4598.5(3)	1438.09(13)
Z	4	4	2
d_{calc}/(g·cm^{-3})	1.779	1.603	1.925
μ/mm^{-1}	6.967	5.778	9.152
F(0 0 0)	1992.0	2168.0	782
Crystal size/mm^3	0.15 × 0.15 × 0.1	0.287 × 0.206 × 0.121	0.43 × 0.40 × 0.20
Radiation	MoKα (λ = 0.71073)	MoKα (λ = 0.71073)	MoKα (λ = 0.71073)
2Θ range for data collection/°	1.928–57.738	3.36–61.98	2.928–51.924
Index ranges	$-15 \le h \le 15$, $-18 \le k \le 21$, $-27 \le l \le 27$	$-19 \le h \le 20$, $-29 \le k \le 29$, $-21 \le l \le 21$	$-10 \le h \le 10$, $-14 \le k \le 14$, $-17 \le l \le 18$
Reflections collected	35,341	49,223	14,571
Uniq. refl./R(int)/R(sigma)	16213/0.0528/0.0956	12944/0.0414/0.0469	5619/0.0500/0.0702
Data/restraints/parameters	16213/0/835	12944/6/551	5619/13/283
Goodness-of-fit on F^2	0.973	1.043	1.045
Final R_1 [I > = 2σ (I)]	0.0473	0.0320	0.0427
Final R_1, wR_2 [all data]	0.0958, 0.0928	0.0492, 0.0833	0.0663, 0.1126
$\Delta\rho_{min}/\Delta\rho_{max}$ (e/Å^3)	3.44/-1.90	1.57/-1.01	−0.78/1.31

consistent with the electron-donating ability of the phosphite ligands (Table 5). This trend holds for all types of complexes (diphosphite (***a***), phosphite-phosphine (***b***), and phosphite-carbonyl (***c***)), *i.e.*, the $E_{1/2}$ values shifted to the anodic region in the order **1a** < **2a** < **3a**, **1b** < **2b** < **3b**, and **1c** < **2c** < **3c**. A cathodic shift of the $E_{1/2}$ values upon the replacement of one phosphite ligand in the complexes of type ***a*** by more electron-donor PPh_3 ligand would be expected. However, only the $P(OPh)_3$-complexes behaved in accordance with this assumption; on going from the complexes **1a** and **2a** to **1b** and **2b** the anodic shift of the first redox potentials were observed (Table 5). On the other hand, if we move from the bisphosphine complex **4** replacing one PPh_3 by the less σ-donor phosphite ligands the expected anodic shift of the $E_{1/2}$ values would be obtained.

The first oxidation and reduction potentials values of **1c–3c**, **5** significantly shifted in the anodic area in comparison with those of the type ***a*** and ***b*** complexes (Table 5) that is a result of substitution of one of the Pt-bound phosphorus-donor ligand in the RePt complexes by π-acceptor CO group. This shift is more pronounced for the complex **3c**, which contains the weaker σ-donor $P(OPh)_3$ ligand. Introduction of the CO ligand in coordination environment of the Pt atom also caused a change in schemes of redox transformations of the complexes **1c–3c**, **5** compared to that with both phosphorous-donor ligands (**1a–3b**, **4**).

The half wave oxidation potential value of the third (**1a–3a**, **4**) or the second oxidation stage (**1b-3b**) of the complexes with two phosphorous-donor ligands (Table 5, Fig. 2a, peak A_2; Fig. 2b, peak B_2) coincides with the oxidation potential value ($E_{1/2}$ = 0.33 V) of the mononuclear rhenium vinylidene complex (Table 5, Fig. 2d, peak D_1) [48,49]. This demonstrates that the one-electron oxidation of the binuclear RePt complexes (**1a–3b**, **4**) results in decomposition of those to $Cp(CO)_2Re{=}C{=}CHPh$. In contrast to **1a–3b**, **4** no oxidation peaks of the rhenium vinylidene at the cyclic voltammograms were detected for the complexes (**1c–3c**) containing the Pt-bound CO group (Fig. 2c). Moreover, the first one-electron oxidation wave of tricarbonyl μ-vinylidene RePt species at the GC electrode is quasi-reversible[2], indicating their greater electrochemical stability relative to **1a–3b**, **4**. Thus, the one-electron oxidation process of **1c–3c**, **5** is quasi-reversible and the following scheme of their oxidation is to be proposed:

$$Cp(CO)_2RePt(\mu\text{-}C{=}CHPh)L(CO) \underset{+\bar{e}}{\overset{-\bar{e}}{\rightleftarrows}} [Cp(CO)_2RePt(\mu\text{-}C{=}CHPh)L(CO)]^{+\cdot}$$

Aside from the oxidation wave with $E_{1/2}$ = 0.33 V, the cyclic voltammograms of the type ***a*** complexes and **4** at the Pt electrode contain a small oxidation wave with $E_{1/2}$ = 0.26 V[3] (n < 1) (Fig. 3), its potential value is similar to those of μ-divinylidene complex $Cp(CO)_2Re{=}C{=}C(Ph){-}C(Ph){=}C{=}Re(CO)_2Cp$, which electrochemistry was studied by Ustynyuk's group in detail [49]. To gain insight into a way of the formation of this μ-divinylidene compound in CV conditions the controlled potential electrolysis of **1a–3b**, **4** with a working platinum electrode and their reactions with $[Cp_2Fe][BF_4]$ were performed.

Controlled potential electrolysis of acetonitrile solutions of the complexes of type ***a*** and ***b*** at their first oxidation wave with the following TLC separation and IR identification of the post-electrolysis solution showed the formation of both mononuclear vinylidene and μ-divinylidene rhenium species as main products. At the same time, only $Cp(CO)_2Re{=}C{=}CHPh$ was detected after the chemical oxidation of **1a–3b**, **4** solutions both in dichloromethane and in acetonitrile. Therefore, the binuclear RePt complexes (**1a–3b**, **4**) undergoes one-electron oxidation with a cleavage of the Re-Pt and Pt-C bonds, and the following schemes of oxidation of **1a–3b**, **4** can be proposed:

[2] The ratio of cathodic to anodic peak currents I_{pc}/I_{pa} = 0.76 (I_{pc} = 60, I_{pa} = 79), $\Delta E = |E_{pa} - E_{pc}|$ = 0.576 mV (Fig. 2c, peaks C_1, C_1')

[3] The absence of the wave with $E_{1/2}$ = 0.26 V on the cyclic voltammograms of types ***a*** and ***b*** complexes at GC-electrode and of type ***b*** complexes at Pt electrode can be explained by coalescence of that wave with the next wave ($E_{1/2}$ = 0.33 V)

$$Cp(CO)_2RePt(\mu - C{=}CHPh)(L)(L') \xrightarrow{-\bar{e}} [Cp(CO)_2RePt(\mu - C{=}CHPh)(L)(L')]^{+\bullet} \rightarrow Cp(CO)_2Re = C{=}\ CHPh\ + [Pt(L)(L')]^{+\bullet}$$

However, in the CV and the CPE conditions especially with a working platinum electrode the process of the cleavage of the Re-Pt and Pt-C bonds can proceed by two pathways. One of them resulted in formation of $Cp(CO)_2Re{=}C{=}CHPh$ and $[PtL_2]^{+\bullet}$ fragment, the other in the neutral $[PtL_2]_{solv}$ fragment and cation-radical of the rhenium complex $[Cp(CO)_2Re{=}C{=}CHPh]^{+\bullet}$:

$$Cp(CO)_2RePt(\mu - C{=}CHPh)(L)(L') \xrightarrow{-\bar{e}} [Cp(CO)_2RePt(\mu - C{=}CHPh)(L)(L')]^{+\bullet} \rightarrow [Cp(CO)_2Re{=}C{=}CHPh]^{+\bullet} + [Pt(L)(L')]$$

This cation-radical seems to undergo some transformations on the electrode surface leading to a generation of the bis-vinylidene rhenium complex. It is noteworthy that previously the formation of $Cp(CO)_2Re{=}C{=}C(Ph){-}C(Ph){=}C{=}Re(CO)_2Cp$ under the CV conditions was not observed, in contrast to its manganese analog [50]. The bis-vinylidene rhenium complex was shown to be generated only under the treatment of $Cp(CO)_2Re{=}C{=}CHPh$ with $[(\eta^5\text{-}C_5H_5)_2Fe]BF_4$/triethylamine couple in dichloromethane at room temperature [49]. Moreover, the controlled potential electrolysis at a Pt-electrode of μ-vinylidene RePt and RePd complexes with chelate diphosphine ligands resulted in only the formation of $Cp(CO)_2Re{=}C{=}CHPh$, the second pathway yielding the rhenium cation-radical $[Cp(CO)_2Re{=}C{=}CHPh]^{+\bullet}$ and its dehydrodimerization product $Cp(CO)_2Re{=}C{=}C(Ph){-}C(Ph){=}C{=}Re(CO)_2Cp$ wasn't observed at all [38,48,51]. Therefore, the formation of $Cp(CO)_2Re{=}C{=}C(Ph){-}C(Ph){=}C{=}Re(CO)_2Cp$ under the electrochemical conditions can be explained by specific behavior of the generated cation radicals $[Cp(CO)_2Re{=}C{=}CHPh]^{+\bullet}$ and the platinum fragments on the surface of the platinum electrode.

Table 4
Comparison of geometric parameters of $Cp(CO)_2RePt(\mu\text{-}C{=}CHPh)[P(OPr^i)_3]L$ [L = $[P(OPr^i)_3]$ (**1a**), PPh_3 (**1b**), CO (**1c**)].

	1a $[P(OPr^i)_3]_2$	**1b** $[P(OPr^i)_3](PPh_3)$	**1c** $[P(OPr^i)_3](CO)$
Bond length (Å)			
Re-Pt	2.7154(5)	2.7337(2)	2.7281(5)
	2.7242(5)		
Re-C1	2.102(8)	2.102(4)	2.076(9)
	2.074(8)		
Pt-C1	2.006(8)	1.998(4)	1.993(9)
	2.016(8)		
C1═C2	1.341(10)	1.334(6)	1.348(12)
	1.348(10)		
Pt-P1	2.221(2)	2.2196(11)	2.241(3)
	2.217(2)		
Pt-P2	2.299(2)	2.3442(11)	–
	2.297(2)		
Pt-C5	–	–	1.921(13)
C5-O5	–	–	1.129(13)
Re-C3	1.890(10)	1.907(5)	1.910(12)
	1.888(9)		
C3-O3	1.187(10)	1.162(6)	1.162(12)
	1.174(9)		
Re-C4	1.886(9)	1.900(5)	1.877(12)
	1.899(10)		
C4-O4	1.158(10)	1.151(5)	1.165(12)
	1.161(10)		
Pt-C3	2.772(10)	2.709(4)	2.712(9)
	2.837(10)		
Bond angle (°)			
Re-C1-Pt	82.7(3)	83.59(16)	84.2(3)
	83.5(3)		
Pt-Re-C1	47.1(2)	46.59(11)	46.6(3)
	47.3(2)		
Re-Pt-C1	50.2(2)	49.82(12)	49.2(3)
	49.1(2)		
Re-C1-C2	143.0(7)	143.8(3)	141.4(8)
	143.9(7)		
Pt-C1-C2	134.0(6)	132.6(3)	134.1(8)
	132.4(7)		
P1-Pt-Re	150.55(6)	152.15(3)	147.78(7)
	151.19(6)		
P2-Pt-Re	105.48(6)	111.87(3)	
	107.23(6)		
C5-Pt-Re	–	–	114.1(4)
Re-C3-O3	174.5(7)	173.8(4)	168(1)
	172.3(7)		
Re-C4-O4	179.0(8)	178.3(4)	178(1)
	178.7(8)		
Pt-C5-O5	–	–	178(1)
P1-Pt-P2	103.06(7)	95.34(4)	
	101.31(7)		
P1-Pt-C5	–	–	97.2(4)
Dihedral angle (°)			
ReC1Pt/C1C2C6	3.4(5)	1.9(3)	8.(2)
Torsion angle (°)			
C7-C6-C2-C1	1.2(2)	8.8(8)	−21.5(13)

3. Conclusion

In this article, two main synthetic approaches have been utilized to prepare binuclear μ-vinylidene RePt complexes with terminal phosphite ligands at the Pt atom: (i) a consecutive addition of metal-containing

Table 5
Electrochemistry data of the complexes **1a–3c**, **4**, **5**, $Cp(CO)_2Re{=}C{=}CHPh$ (MeCN, 0.1 M Et_4NBF_4, 2 mM, Ag/0.1 M $AgNO_3$ in MeCN).

Compounds	$E_{1/2}$, V (n)		
	Oxidation		Reduction
	Pt	GC	DME
$Cp(CO)_2Re(\mu\text{-}C{=}CHPh)Pt[P(OPr^i)_3]_2$ (**1a**)	−0.12(1)	−0.07(1)	−2.87(1)
	0.26(< 1)	0.35(< 1)	
	0.33(< 1)		
$Cp(CO)_2RePt(\mu\text{-}C{=}CHPh)[P(OEt)_3]_2$ (**2a**)	−0.06(1)	−0.03(1)	−2.83(1)
	0.26(< 1)	0.38(< 1)	−3.06(1)
	0.32(< 1)		
$Cp(CO)_2RePt(\mu\text{-}C{=}CHPh)[P(OPh)_3]_2$ (**3a**)	0.12(1)	0.14(1)	−2.70(1)
	0.26(< 1)	0.39(< 1)	−3.05(1)
	0.33(< 1)		
$Cp(CO)_2RePt(\mu\text{-}C{=}CHPh)[P(OPr^i)_3](PPh_3)$ (**1b**)	−0.02(1)	0.01(1)	−2.82(1)
	0.36(< 1)	0.38(< 1)	−2.92(1)
			−3.05(1)
$Cp(CO)_2RePt(\mu\text{-}C{=}CHPh)[P(OEt)_3](PPh_3)$ (**2b**)	−0.01(1)	0.04(1)	−2.81(1)
	0.36(< 1)	0.38(< 1)	−3.05(1)
$Cp(CO)_2RePt(\mu\text{-}C{=}CHPh)[P(OPh)_3](PPh_3)$ (**3b**)	0.02(1)	0.06(1)	−2.69(1)
	0.36(< 1)	0.36(< 1)	
$Cp(CO)_2RePt(\mu\text{-}C{=}CHPh)[P(OPr^i)_3](CO)$ (**1c**)	0.22(1)	0.26(1)[a]	−2.47(1)
			−2.71(1)
			−3.00(1)
$Cp(CO)_2RePt(\mu\text{-}C{=}CHPh)[P(OEt)_3](CO)$ (**2c**)	0.24(1)	0.28(1)[a]	−2.45(1)
			−2.82(1)
$Cp(CO)_2RePt(\mu\text{-}C{=}CHPh)[P(OPh)_3](CO)$ (**3c**)	0.30(1)	0.32(1)[a]	−2.31(1)
$Cp(CO)_2RePt(\mu\text{-}C{=}CHPh)(PPh_3)_2$ (**4**)	−0.07(1)	0.00(1)	−2.60(1)
	0.26(< 1)	0.29(< 1)	−2.80(1)
	0.33(< 1)	0.36(< 1)	−3.00(1)
$Cp(CO)_2RePt(\mu\text{-}C{=}CHPh)(PPh_3)(CO)$ (**5**)	0.17(1)[a]	0.18(1)[a]	−2.33(1)[a]
	1.07(< 1)	1.02(< 1)	−3.00(1)
$Cp(CO)_2Re{=}C{=}CHPh$	0.33(1)	0.36(1)	−2.21(1)
			−2.82(1)

[a] The quasi-reversible stage; n – the number of electrons transferred in a particular electrochemical stage (the number of the electrons n < 1 indicates that the wave height is smaller than the height of the one-electron wave).

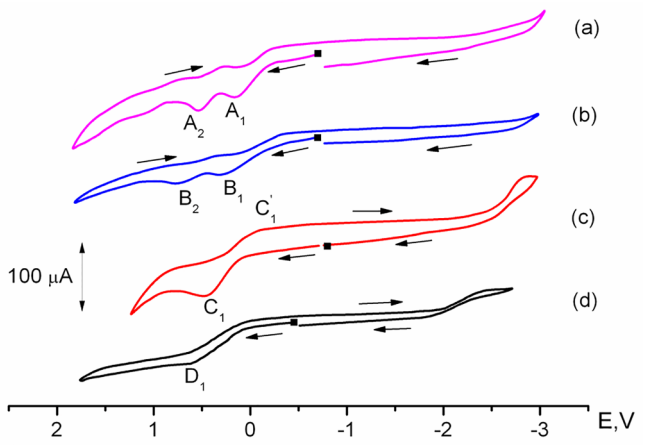

Fig. 2. The cyclic voltammograms of complexes: ***(a)*** – $Cp(CO)_2RePt(\mu\text{-}C{=}CHPh)[P(OEt)_3]_2$ (**2a**), ***(b)*** – $Cp(CO)_2RePt(\mu\text{-}C{=}CHPh)[P(OEt)_3](PPh_3)$ (**2b**), ***(c)*** – $Cp(CO)_2RePt(\mu\text{-}C{=}CHPh)[P(OEt)_3](CO)$ (**2c**), ***(d)*** – $Cp(CO)_2Re{=}C{=}CHPh$, at GC-electrode in MeCN (0.1 M Et_4NBF_4, C = 2 mM, scan rate 25 mV s^{-1}, potentials vs. Ag/0.1 M $AgNO_3$ in MeCN).

fragments to the rhenium vinylidene; (ii) ligand substitution or exchange reactions at the Pt atom in the μ-vinylidene complexes with RePt core. A series of the new binuclear μ-vinylidene complexes $Cp(CO)_2RePt(\mu\text{-}C{=}CHPh)LL'$ (L = L′ = $P(OPr^i)_3$ (**1a**), $P(OEt)_3$ (**2a**), $P(OPh)_3$ (**3a**); L′ = PPh_3, L = $P(OPr^i)_3$ (**1b**), $P(OEt)_3$ (**2b**), $P(OPh)_3$ (**3b**)) were obtained by means of different methods. An applicability of certain method depends on the nature $P(OR)_3$ ligand that we would like to introduce into the binuclear complex. For example, the most convenient methods to complexes **1a** and **2a** is based on the reactions of $[Cp(CO)_2RePt(\mu\text{-}C{=}CHPh)(PPh_3)_2]$ (**4**) with free phosphites and to complex **3a** based on the treatment of $Cp(CO)_2Re{=}C{=}CHPh$ with $Pt[P(OPh)_3]_4$. The mixed ligand complexes **1b** and **2b** were obtained in high yields by the interaction between $Cp(CO)_2RePt(\mu\text{-}C{=}CHPh)(PPh_3)_2$(**4**) and $Cp(CO)_2RePt(\mu\text{-}C{=}CHPh)[P(OR)_3]_2$ (**1a**, **2a**). The best yield for $Cp(CO)_2RePt(\mu\text{-}C{=}CHPh)(PPh_3)[P(OPh)_3]$ (**3b**) was reached by the reaction of $Cp(CO)_2Re{=}C{=}CHPh$ with mixed ligand species $Pt(PPh_3)_3[P(OPh)_3]$.

We also studied the possibility of substitution of the phosphorous-donor ligands at the platinum atom in the obtained binuclear vinylidenes by carbon monoxide. The reactions of the type ***a*** and ***b*** complexes with $Co_2(CO)_8$ were shown to result in the selective substitution of the Pt-bound phosphite or phosphine ligand being *trans to* the bridging vinylidene to give $Cp(CO)_2RePt(\mu\text{-}C{=}CHPh)(CO)L$ [L = $P(OPr^i)_3$ (**1c**), $P(OEt)_3$ (**2c**), $P(OPh)_3$ (**3c**)].

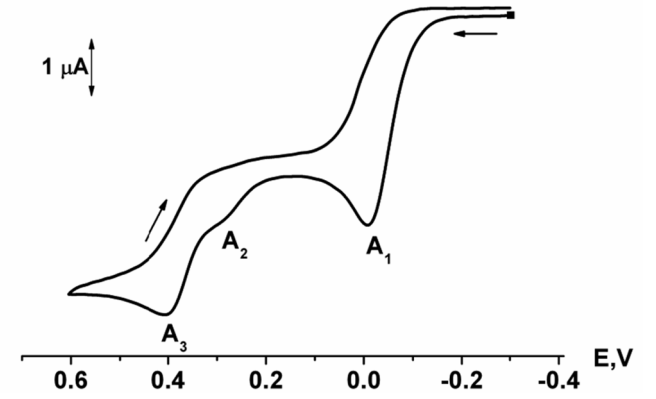

Fig. 3. The cyclic voltammogram of $Cp(CO)_2RePt(\mu\text{-}C{=}CHPh)[P(OEt)_3]_2$ (**2a**) at Pt-electrode in MeCN (0.1 M Et_4NBF_4, C = 2 mM, scan rate 25 mV s^{-1}, potentials vs. Ag/0.1 M $AgNO_3$ in MeCN).

The XRD, IR and NMR spectroscopy, and electrochemical study of complexes **1a–3c** revealed an influence of a ligand environment of the platinum atom on the properties of the synthesized compounds. Such influence is minor in the structural and spectroscopic characteristics of the complexes, whereas a strong difference is detected in the electrochemical behavior between the type c complexes and the others. So, the introduction of π-acceptor CO ligand in the RePt vinylidene complexes resulted in increasing of electrochemical stability of **1c–3c** as indicated by their quasi-reversible first one electron oxidation wave. On the other hand, one-electron oxidation of **1a–3b** resulted in their decomposition to the $Cp(CO)_2Re{=}C{=}CHPh$ complex and $[PtL_2]^{+\cdot}$ fragment.

4. Experimental

4.1. General considerations

All operations and manipulations were carried out under an argon atmosphere. Solvents were purified by distillation from appropriate drying agents and stored under argon. The course of reactions was monitored by TLC on Silufol plates and IR spectroscopy. Neutral alumina was used for column chromatography. Physical-chemical characteristics were obtained in the Krasnoyarsk Regional Centre of Research Equipment, Siberian Branch of the RussianAcademy of Sciences. The IR spectra were recorded on the Tensor 27 spectrometer (Bruker, Germany). The ^1H, $^{13}C\{^1H\}$ and $^{31}P\{^1H\}$ NMR spectra were obtained using NMR spectrometer AVANCE III 600 (Bruker, Germany). The X-ray data for **1c** were obtained with the Smart Photon II diffractometer, for **1a** with an automatic Bruker X8 Apex diffractometer equipped with a two-dimensional CCD detector (Bruker AXS, Germany). The initial compounds $P(OPr^i)_3$, $P(OEt)_3$ [52], and $Cp(CO)_2RePt(\mu\text{-}C{=}CHPh)(PPh_3)_2$ [36] were synthesized according to published procedures. In the experimental part the synthetic procedures to the complexes **1a–3c** providing the highest yields are described, the rest of the reactions and the NMR spectra of the type ***b*** complexes are included in supplementary data. To avoid repetitions, the ^{31}P NMR spectra data of the complexes **1a–3c** given in Table 3 aren't include in the experimental part.

4.2. Electrochemical study

The electrochemical measurements were carried out in acetonitrile solutions with 0.1 M $[Et_4N][BF_4]$ as a supporting electrolyte. The cyclic voltammograms and polarograms were recorded on an IPC-Pro M potentiostat (Volta, Saint-Petersburg, Russia) using a three-electrode system. The working electrode was a stationary platinum electrode of 1 mm diameter or a stationary glassy carbon (GC) electrode of 4 mm diameter in a Teflon housings or a dropping mercury electrode (DME) with a positive margin drop (m = 3.6 mg/s, τ = 0.23 s). The reference electrode was Ag/0.1 M $AgNO_3$ in MeCN. Potentials are given versus Ag/0.1 M $AgNO_3$ in MeCN (they can be converted to *V* versus *SCE* by adding 0.337 V). The auxiliary electrode was a platinum wire. The reference electrode and the auxiliary electrode were separated from the bulk solution in a glass tube filled with an electrolyte solution and fitted with a porous plug. The number of the electrons transferred in a particular redox process was estimated by comparison of the wave height observed with those of the one-electron ferrocene$^{+/0}$ or $Cp(CO)_2Re{=}C{=}CHPh$ of the same concentration as well as through usual diagnostic electrochemical parameters. The controlled potential electrolysis was carried out with the IPC-Pro potentiostat using a three-electrode system with a platinum plate of 4 cm^2 as the working electrode.

4.2.1. Syntheses of $Cp(CO)_2RePt(\mu\text{-}C{=}CHPh)[P(OPr^i)_3]_2$ (1a)

4.2.1.1. Reaction of $Cp(CO)_2Re{=}C{=}CHPh$ with $Pt[P(OPr^i)_3]_4$. A mixture of 50 mg (0.122 mmole) of $Cp(CO)_2Re{=}C{=}CHPh$ and 125 mg (0.122 mmole) of $Pt[P(OPr^i)_3]_4$ in 10 mL of benzene was

stirred for 4 h. The resultant solution was dried *in vacuo* and the obtained yellow residue was dissolved in 5 mL hexane–benzene mixture (1:1) and chromatographed on an alumina column (8 × 2 cm). The column was eluted initially with hexane–benzene (9:1), (4:1) and (1:1) mixture. The first colorless zone contained $P(OPr^i)_3$ and $Cp(CO)_2Re[\eta^2$-$HC(P(=O)(OPr^i)_2)=CHPh]$, identified by IR. The second yellow major band, after removal of solvent and crystallization from hexane, afforded yellow microcrystals of **1a**. Yield: 75 mg, 60%.

4.2.1.2. Reaction of $Cp(CO)_2RePt(\mu$-$C=CHPh)(PPh_3)_2$ (4) with $P(OPr^i)_3$. $P(OPr^i)_3$ (109 mg, 0.525 mmol) was added to a solution of $[Cp(CO)_2RePt(\mu$-$C=CHPh)(PPh_3)_2]$ (**4**) (109 mg, 0.105 mmol) in 10 mL of benzene and reaction mixture was stirred for 12 h. Then the mixture was dried *in vacuo*. A bright-yellow residue was dissolved in hexane–benzene mixture (1:1) and chromatographed on an alumina column (8 × 2 cm). The column was eluted initially with hexane–benzene (2:1) mixture and subsequently with benzene. The first colorless zone contained PPh_3 and $P(OPr^i)_3$. The second yellow major band, after removal of solvent and crystallization from benzene-hexane mixture (1:1), afforded yellow microcrystals of **1a**. Yield: 71 mg, 85%.

*4.2.1.3. $Cp(CO)_2RePt(\mu$-$C=CHPh)[P(OPr^i)_3]_2$ (**1a**). Anal.* Found: C, 39.01; H, 5.20%. Calc. for $C_{33}H_{53}O_8P_2PtRe$ (1021.00): C, 38.82; H, 5.23%.

IR (cm^{-1}): 1943 s, 1873 s (CH_2Cl_2); 1946 s, 1869 s (tabl. KBr).

^1H NMR (CD_2Cl_2, 25 °C) δ, ppm [*J*, Hz]: 1.38 (d, 18H, ^3J = 6.24, CH_3); 1.40 (d, 18H, ^3J = 6.24, CH_3); 4.88 (m, 6H, CH); 5.34 (s, 5H, C_5H_5); 7.12 (tr, ^3J = 7.29, H_{para} of CH*Ph*); 7.31 (tr, 2H, ^3J = 7.71, H_{meta} of CH*Ph*); 7.66 (d, 2H, ^3J = 7.89, H_{ortho} of CH*Ph*); 8.42 (ddd, $^4J_{PH}$ = 22.37, $^4J_{PH}$ = 14.49, $^3J_{PtH}$ = 14.76, =CH).

$^{13}C\{^1H\}$ NMR (C_6D_6, 25 °C) δ, ppm [*J*, Hz]: 23.91 (d, $^3J_{PC}$ = 7.37, CH_3); 24.17 (br. s, CH_3); 68.28 (d, $^2J_{PtC}$ = 11.00, CH_2); 69.49 (d, $^2J_{PtC}$ = 19.44, CH_2); 85.53 (s, C_5H_5); 123.65 (s, C_{para} of C_6H_5); 126.29 (s, C_{meta} of C_6H_5); 127.70 (s, C_{ortho} of C_6H_5); 138.37 (ddd, $^3J_{PC}$ = 6.06, $^3J_{PC}$ = 2.75, $^2J_{PtC}$ = 108.21, $=C^2H$); 143.10 (dd, $^4J_{PC}$ = 21.46, $^4J_{PC}$ = 9.36, C_{ipso} of C_6H_5); 201.97 (br. s, CO); 228.00 (ddd, $^2J_{PC}$ = 92.80, $^2J_{PC}$ = 4.77, J_{PtC} = 790.82, μ-C^1 =).

*4.2.2. Syntheses of $Cp(CO)_2RePt(\mu$-$C=CHPh)[P(OEt)_3]_2$ (**2a**)*

Complex **2a** was obtained as a pale yellow solid with 65% yield, from reaction of $[Cp(CO)_2RePt(\mu$-$C=CHPh)(PPh_3)_2]$ (**4**) and $P(OEt)_3$ following the procedure **B** used for preparation of complex **1a**.

Anal. Found: C, 34.68; H, 4.45%. Calc. for $C_{27}H_{41}O_8P_2PtRe$ (936.84): C, 34.62; H, 4.41%.

IR (cm^{-1}): 1940 s, 1870 s (CH_2Cl_2); 1932 s, 1869 s (tabl. KBr).

^1H NMR (C_6D_6, 25 °C) δ, ppm [*J*, Hz]: 1.10 (tr, 9H, ^3J = 7.10, CH_3); 1.20 (tr, 9H, ^3J = 7.10, CH_3); 3.99 (dkv, 6H, ^3J = 7.10, $^3J_{PH}$ = 8.24, CH_2); 4.06 (dkv, 6H, ^3J = 7.10, $^3J_{PH}$ = 7.32, CH_2); 5.08 (s, 5H, C_5H_5); 7.15 (tr, ^3J = 7.33, H_{para} of CH*Ph*); 7.37 (tr, 2H, ^3J = 8.01, H_{meta} of CH*Ph*); 7.99 (dd, 2H, ^3J = 8.01, H_{ortho} of CH*Ph*); 8.90 (ddd, $^4J_{PH}$ = 23.35, $^4J_{PH}$ = 15.33, $^3J_{PtH}$ = 15.79, =CH).

$^{13}C\{^1H\}$ NMR (C_6D_6, 25 °C) δ, ppm [*J*, Hz]: 15.79 (d, $^3J_{PC}$ = 7.37, CH_3); 16.09 (d, $^3J_{PC}$ = 6.50, CH_3); 60.07 (d, $^2J_{PtC}$ = 13.00, CH_2); 60.37 (d, $^2J_{PtC}$ = 20.37, CH_2); 85.07 (s, C_5H_5); 124.02 (s, C_{para} of C_6H_5); 126.71 (s, C_{meta} of C_6H_5); 127.93 (s, C_{ortho} of C_6H_5); 138.48 (ddd, $^3J_{PC}$ = 5.20, $^3J_{PC}$ = 2.60, $^2J_{PtC}$ = 109.02, $=C^2H$); 143.75 (dd, $^4J_{PC}$ = 21.67, $^4J_{PC}$ = 9.54, C_{ipso} of C_6H_5); 202.07 (s, 2CO); 228.80 (ddd, $^2J_{PC}$ = 93.63, $^2J_{PC}$ = 5.20, J_{PtC} = 791.77, μ-C^1 =).

*4.2.3. Syntheses of $Cp(CO)_2RePt(\mu$-$C=CHPh)[P(OPh)_3]_2$ (**3a**)*

Complex $Cp(CO)_2RePt(\mu$-$C=CHPh)[P(OPh)_3]_2$ (**3a**) was obtained similar to procedure **A** for complex **1a** using $Pt[P(OPh)_3]_4$ instead of $Pt[P(OPr^i)_3]_4$: A mixture of 50 mg (0.122 mmole) of $Cp(CO)_2Re=C=CHPh$ and 175 mg (0.122 mmole) of $Pt[P(OPh)_3]_4$ in 10 mL of benzene was stirred for 24 h. The resultant solution was dried *in vacuo* and the obtained yellow residue was dissolved in 5 mL hexane–benzene mixture (1:1) and chromatographed on an alumina column (8 × 2 cm). The column was eluted initially with hexane–benzene (4:1) and (1:1) mixture. The first colorless zone contained $P(OPh)_3$. The second yellow major band, after removal of solvent and crystallization from diethyl ether, afforded yellow microcrystals of **3a**. Yield: 119 mg, 80%.

Anal. Found: C, 50.68; H, 3.85%. Calc. for $C_{51}H_{41}O_8P_2PtRe$ (1225.10): C, 50.00; H, 3.37%.

IR (cm^{-1}): 1952 s, 1881 s (CH_2Cl_2), 1947 s, 1877 s (tabl. KBr).

^1H NMR ($CDCl_3$, 25 °C) δ, ppm [*J*, Hz]: 4.83 (s, 5H, C_5H_5); 7.05–7.31 (H_{para},H_{meta},H_{ortho} of Ph); 8.32 (ddd, $^4J_{PH}$ = 25.30,$^4J_{PH}$ = 15.68,$^3J_{PtH}$ = 18.76, =CH).

$^{13}C\{^1H\}$ NMR ($CDCl_3$, 25 °C) δ, ppm [*J*, Hz]: 85.88 (s, C_5H_5); 120.80 (d, $^5J_{PC}$ = 5.20, C_{para} of OC_6H_5); 121.32 (d, $^5J_{PC}$ = 5.20, C_{para} of OC_6H_5); 124.10 (s, C_{para} of C_6H_5); 124.26 (s, C_{meta} of OC_6H_5); 124.40 (s, C_{meta} of OC_6H_5); 126.61 (s, C_{meta} of C_6H_5); 127.53 (s, C_{ortho} of C_6H_5); 129.03 (s, C_{ortho} of OC_6H_5); 129.36 (s, C_{ortho} of OC_6H_5); 140.55 (dd, $^3J_{PC}$ = 4.16, $^2J_{PtC}$ = 102.65, $=C^2H$); 142.96 (dd, $^4J_{PC}$ = 22.37, $^4J_{PC}$ = 9.89, C_{ipso} of C_6H_5); 151.31 (d, $^2J_{PC}$ = 6.24, C_{ipso} of OC_6H_5); 151.49 (d, $^2J_{PC}$ = 5.55, C_{ipso} of OC_6H_5); 229.49 (dd, $^2J_{PC}$ = 92.25, J_{PtC} = 781.66, μ-C^1 =).

*4.2.4. Syntheses of $Cp(CO)_2RePt(\mu$-$C=CHPh)[P(OPr^i)_3](PPh_3)$ (**1b**)*

4.2.4.1. Reaction of $Cp(CO)_2RePt(\mu$-$C=CHPh)[P(OPr^i)_3]_2$ (1a) with an excess of PPh_3. PPh_3 (175 mg, 0.668 mmol) was added to a solution of $Cp(CO)_2RePt(\mu$-$C=CHPh)[P(OPr^i)_3]_2$ (**1a**) (127 mg, 0.125 mmol) in 10 mL of benzene. The mixture after being stirred for 8 h was dried *in vacuo*. A bright-yellow residue was dissolved in hexane–benzene mixture (1:1) and chromatographed on an alumina column (6 × 2 cm). The column was eluted initially with hexane, hexane–benzene (4:1) mixture and subsequently with hexane–benzene (1:1) mixture. The first colorless eluate contained PPh_3 and $P(OPr^i)_3$. The second yellow major band, after removal of solvent and crystallization from hexane, gave83 mg of unreacted **1a**. The third bright-yellow band, after removal of solvent and crystallization from benzene-hexane mixture (1:5), yield 46 mg (34%) of **1b**.

4.2.4.2. Reaction of $Cp(CO)_2RePt(\mu$-$C=CHPh)(PPh_3)_2$(4) with one equivalent of $P(OPr^i)_3$. $P(OPr^i)_3$ (9 mg, 0.044 mmol) was added to a solution of $Cp(CO)_2RePt(\mu$-$C=CHPh)(PPh_3)_2$ (**4**) (50 mg, 0.044 mmol) in 10 mL of benzene and reaction mixture was stirred for 20 min. The mixture after being stirred for 30 min was dried*in vacuo*. A bright-yellow residue was dissolved in hexane–benzene mixture (1:1) and chromatographed on an alumina column (8 × 2 cm). The column was eluted initially with hexane–benzene (2:1) mixture and subsequently with benzene. The first colorless zone contained PPh_3. The second yellow major band, after removal of solvent and crystallization from benzene-hexane mixture (1:1), afforded yellow microcrystals of **1b**. Yield: 31 mg, 65%. The third yellow band after removal of solvent afforded 10 mg (21%) orange microcrystals of unreacted **4**.

4.2.4.3. Reaction between $Cp(CO)_2RePt(\mu$-$C=CHPh)[P(OPr^i)_3]_2$ (1a) and $Cp(CO)_2RePt(\mu$-$C=CHPh)(PPh_3)_2$(4). A mixture of $Cp(CO)_2RePt(\mu$-$C=CHPh)(PPh_3)_2$ (**4**) (22 mg, 0.020 mmole) and $Cp(CO)_2RePt(\mu$-$C=CHPh)[P(OPr^i)_3]_2$ (**1a**) (20 mg, 0.020 mmol) in 0.1 mL of benzene was heated at 60 °C. The solution after being stirred for 5 h was cooled to RT and dried *in vacuo*. The obtained bright-yellow oiled residue was crystallized from Et_2O-hexane mixture (1:2) and afforded orange microcrystals of **1b**. Yield: 30 mg, 70%.

Anal. Found: C, 46.83; H, 4.36%. Calc. for $C_{42}H_{47}O_5P_2PtRe$ (1075.05): C, 46.92; H, 4.41%.

IR (cm^{-1}): 1935 s, 1859 s (CH_2Cl_2); 1922 s, 1851 s (tabl. KBr).

^1H NMR (CD_2Cl_2, 25 °C) δ, ppm [*J*, Hz]:1.11 (br, 18H, CH_3); 4.73 (br, 3H, CH); 4.86 (s, 5H, C_5H_5); 7.11 (tr, ^3J = 7.29, H_{para} of CH*Ph*); 7.30 (tr, ^3J = 7.61, H_{para} of PPh_3); 7.46 (m, H_{meta} of CH*Ph* and PPh_3); 7.65 (d, ^3J = 7.70, H_{ortho} of CH*Ph*); 7.76 (d, ^3J = 8.53, H_{ortho} of PPh_3);

7.77 (d, ^3J = 8.62, H_{ortho} of PPh_3); 8.49 (ddd, $^4J_{PH} \approx {}^4J_{PH}$ = 15.09, $^3J_{PtH}$ = 7.32, =CH).

$^{13}C\{^1H\}$ NMR (CD_2Cl_2, 25 °C) δ, ppm [J, Hz]: 23.53 (d, $^3J_{PC}$ = 4.03, CH_3); 69.06 (d, $^2J_{PtC}$ = 18.71, CH); 85.10 (s, C_5H_5); 123.50 (s, C_{para} of C_6H_5); 126.02 (s, C_{meta} of C_6H_5);127.65 (d, $^3J_{PC}$ = 9.54, C_{meta} of P(C_6H_5)$_3$);127.75 (s, C_{ortho} of C_6H_5);129.33 (d, $^4J_{PC}$ = 1.10, C_{para} of P(C_6H_5)$_3$);134.48 (dd, $^2J_{PC}$ = 12.47, $^3J_{PtC}$ = 13.03, C_{ortho} of P(C_6H_5)$_3$);135.44 (dd, J_{PC} = 38.15, $^2J_{PtC}$ = 17.61, C_{ipso} of P(C_6H_5)$_3$);137.00 (ddd, $^3J_{PC} \approx {}^3J_{PC}$ = 3.30, $^2J_{PtC}$ = 115.18, =C^2H);143.26 (dd, $^4J_{PC}$ = 14.51, $^4J_{PC}$ = 9.72, C_{ipso} of C_6H_5);202.81 (br, s, 2CO);228.02 (dd, $^2J_{PC}$ = 64.01, $^2J_{PC}$ = 6.06, μ-C^1 =).

4.2.5. Syntheses of $Cp(CO)_2RePt(\mu$-C=CHPh)[P(OEt)$_3$](PPh$_3$) (2b)

4.2.5.1. Reaction of $Cp(CO)_2RePt(\mu$-C=CHPh)[P(OEt)$_3$]$_2$ (2a) with an excess of PPh_3.. Complex **2b** was obtained as a bright yellow solid with 65% yield, from reaction of $Cp(CO)_2RePt(\mu$-C=CHPh)[P(OEt)$_3$]$_2$ (**2a**) and PPh_3 following the procedure **A** used for preparation of complex **1b**.

4.2.5.2. Reaction of $Cp(CO)_2RePt(\mu$-C=CHPh)(PPh$_3$)$_2$ (4) with one equivalent of P(OEt)$_3$.. Following the procedure **B** described for preparation of **1b**, complex **2b** was obtained with 67% yield.

4.2.5.3. Reaction between $Cp(CO)_2RePt(\mu$-C=CHPh)[P(OEt)$_3$]$_2$ (2a) and $Cp(CO)_2RePt(\mu$-C = CHPh)(PPh$_3$)$_2$ (4). Interaction of **2a** and **4** resulted in 71% yield of complex **2b** under the same conditions used for preparation of **1b** by method **C**.

Anal. Found: C, 46.48; H, 4.12%. Calc. for $C_{39}H_{41}O_5P_2PtRe$ (1033.16): C, 45.35; H, 4.00%.

IR (cm^{-1}): 1936 s, 1860 s (CH_2Cl_2);1926 s, 1854 s (tabl. KBr).

^1H NMR ($CDCl_3$, 25 °C) δ, ppm [J, Hz]: 0.89 (tr, 9H, ^3J = 7.10, CH_3); 3.90 (dkv, 6H, ^3J = 7.10, $^3J_{HP}$ = 7.44, CH_2); 4.63 (s, 5H, C_5H_5); 7.04–7.12 (m, H_{para} of CH*Ph* and PPh_3); 7.37 (m, H_{meta} of CH*Ph* and PPh_3); 7.82 (d, ^3J = 8.93, H_{ortho} of PPh_3); 7.84 (d, ^3J = 8.36, H_{ortho} of PPh_3); 8.00 (d, ^3J = 7.32, H_{ortho} of CHPh); 8.91 (ddd, $^4J_{PH} \approx {}^4J_{PH}$ = 15.34, $^3J_{PtH}$ = 7.32, =CH).

$^{13}C\{^1H\}$ NMR ($CDCl_3$, 25 °C) δ, ppm [J, Hz]: 15.80 (d, $^3J_{PC}$ = 7.28, CH_3); 60.56 (d, $^2J_{PtC}$ = 20.81, CH_2); 85.03 (s, C_5H_5); 123.56 (s, C_{para} of C_6H_5); 126.23 (s, C_{meta} of C_6H_5); 127.60 (d, $^3J_{PC}$ = 9.71, C_{meta} of P(C_6H_5)$_3$); 127.74 (s, C_{ortho} of C_6H_5); 129.32 (d, $^4J_{PC}$ = 1.73, C_{para} of P(C_6H_5)$_3$); 134.32 (dd, $^2J_{PC}$ = 12.14, $^3J_{PtC}$ = 13.01, C_{ortho} of P(C_6H_5)$_3$); 135.37 (dd, J_{PC} = 38.84, $^2J_{PtC}$ = 17.17, C_{ipso} of P(C_6H_5)$_3$); 136.23 (ddd, $^3J_{PC} \approx {}^3J_{PC}$ = 2.70, $^2J_{PtC}$ = 112.36, =C^2H); 143.53 (dd, $^4J_{PC}$ = 14.74, $^4J_{PC}$ = 10.24, C_{ipso} of C_6H_5); 202.50 (s, 2CO); 227.64 (dd, $^2J_{PC}$ = 62.08, $^2J_{PC}$ = 6.24, μ-C^1 =).

4.2.6. Syntheses of $Cp(CO)_2RePt(\mu$-C=CHPh)[P(OPh)$_3$](PPh$_3$) (3b)

4.2.6.1. Reaction of $Cp(CO)_2RePt(\mu$-C=CHPh)[P(OPh)$_3$]$_2$ (3a) with an excess of PPh_3. Following the procedure **A** described for preparation of **1b**, complex **3b** was obtained with 55% yield.

4.2.6.2. Reaction of $Cp(CO)_2Re$=C=CHPh with $Pt(PPh_3)_3[P(OPh)_3]$. To a solution of 200 mg (0.161 mmole) of $Pt(PPh_3)_4$ in 5 mL of benzene a 46 μL (0.177 mmole) of $P(OPh)_3$ was added. After 10 min a 66 mg (0.161 mmole) of $Cp(CO)_2Re$=C=CHPh was added and the mixture was additionally stirred for a 4 h. The obtained solution was dried *in vacuo* and a bright-yellow residue was dissolved in hexane–benzene mixture (1:1) and chromatographed on an alumina column (8 × 2 cm). The column was eluted initially with hexane–benzene (4:1) mixture and subsequently with hexane–benzene (1:1) mixture. The first colorless zone contained PPh_3. The second yellow major band, after removal of solvent and crystallization from diethyl ether afforded orange microcrystals of **3b**. Yield: 166 mg, 88%.

Anal. Found: C, 52.13; H, 3.60%. Calc. for $C_{51}H_{41}O_5P_2PtRe$ (1177.10): C, 52.04; H, 3.51%.

IR (cm^{-1}): 1945 s, 1873 s (CH_2Cl_2); 1945 s, 1874 s (tabl. KBr).

^1H NMR ($CDCl_3$, 25 °C) δ, ppm [J, Hz]: 4.84 (s, 5H, C_5H_5); 7.08–7.71 (H_{para},H_{meta},H_{ortho} of Ph); 9.04 (ddd, $^4J_{PH} \approx {}^4J_{PH}$ = 15.91, $^3J_{PtH}$ = 14.42, =CH).

$^{13}C\{^1H\}$ NMR ($CDCl_3$, 25 °C) δ, ppm [J, Hz]: 85.13 (s, C_5H_5), 120.63–134.71 (C_{para},C_{meta},C_{ortho} of Ph); 138.76 (d, $^2J_{PtC}$ = 100.92, =C^2H); 143.63 (dd, $^4J_{PC}$ = 25.84, $^4J_{PC}$ = 15.09, C_{ipso} of C_6H_5); 151.61 (m, C_{ipso} of P(C_6H_5)$_3$ and P(OC_6H_5)$_3$); 201.18 (br. s, 2CO); 228.80 (dd, $^2J_{PC}$ = 57.91, $^2J_{PC}$ = 4.86, μ-C^1 =).

4.2.7. Syntheses of $Cp(CO)_2RePt(\mu$-C=CHPh)[P(OR)$_3$](CO) (R = Pr^i (1c), Et (2c), Ph (3c))

To a mixture containing 0.098 mmol of $Cp(CO)_2RePt(\mu$-C=CHPh)[P(OR)$_3$]$_2$ (R = Pr^i (**1a**), Et (**2a**), Ph (**3a**)) and 0.108 mmol (10% excess) of $Co_2(CO)_8$ in argon a 10 mL of benzene was added. The solution was allowed to stir at room temperature for 2 h. The solvent was then removed *in vacuo* and the obtained dark-brown residue was redissolved in hexane–benzene (5:1) mixture and chromatographed on an alumina column (7 × 2 cm). Two fractions were successively eluted with hexane, hexane–benzene (9:1) and (3:2) mixtures. The first brown fraction contained yellow–brown complex $Co_2(CO)_7$[P(OR)$_3$]. The required compounds $Cp(CO)_2RePt(\mu$-C=CHPh)[P(OR)$_3$](CO) were obtained by evaporation of solvent from the second bright-yellow fraction.

$Cp(CO)_2RePt(\mu$-C=CHPh)[P(OPr^i)$_3$](CO)(1c) as an orange crystalline solid from hexane. Yield 88%.

Anal. Found: C, 35.77; H, 3.90%. Calc. For$C_{25}H_{32}O_6PPtRe$ (840,78): C, 35.71; H, 3.84%.

IR (cm^{-1}): 2030 s, 1940 s, 1878 s (CH_2Cl_2); 2027 s, 1932 s, 1872 s (tabl. KBr).

^1H NMR (C_6D_6, 25 °C) δ, ppm [J, Hz]: 1.14 (d, 18H, ^4J = 6.18, CH_3); 4.72 (m, 6H, CH); 4.78 (s, 5H, C_5H_5); 7.10 (tr, ^3J = 7.32, H_{para} of Ph); 7.32 (tr, 2H, ^3J = 7.67, H_{meta} of Ph); 7.89 (d, 2H, ^3J = 8.01, H_{ortho} of Ph); 8.92 (dd, $^4J_{PH}$ = 14.42, $^3J_{PtH}$ = 19.46, =CH).

$^{13}C\{^1H\}$ NMR ($CDCl_3$, 25 °C) δ, ppm [J, Hz]: 23.90 (d, $^3J_{PH}$ = 4.86, CH_3); 70.63 (d, $^3J_{PtH}$ = 19.42, CH); 86.02 (s, C_5H_5); 124.71 (s, C_{para} of C_6H_5); 126.65 (s, C_{meta} of C_6H_5); 127.85 (s, C_{ortho} of C_6H_5); 142.16 (dd, $^3J_{PC}$ = 4.51, $^2J_{PtC}$ = 112.71, =C^2H); 142.52 (dd, $^3J_{PtC}$ = 20.98, $^4J_{PC}$ = 9.36, C_{ipso} of C_6H_5); 195.36 (dd, J_{PtC} = 1217, $^2J_{PC}$ = 1.73, Pt-CO), 227.03 (dd, J_{PtC} = 841, $^2J_{PC}$ = 3.81, μ-C^1 =).

$Cp(CO)_2RePt(\mu$=C=CHPh)[P(OEt)$_3$](CO) (2c) as an orange crystalline solid from hexane. Yield 85%.

Anal. Found: C, 34.15; H, 3.33%. Calc. for $C_{22}H_{26}O_6PPtRe$ (798.70): C, 33.08; H, 3.28%.

IR (cm^{-1}): 2041s, 1939s, 1876m (CH_2Cl_2); 2043s, 1929s, 1869s (tabl. KBr).

^1H NMR (C_6D_6, 25 °C) δ, ppm [J, Hz]: 1.10 (tr, 9H, ^3J = 6.99, CH_3); 3.84 (dkv, 6H, ^3J = 6.99, $^3J_{HP}$ = 8.93, CH_2); 4.78 (s, C_5H_5); 7.09 (tr, ^3J = 7.32, H_{para} of Ph); 7.30 (tr, 2H, ^3J = 7.78, H_{meta} of Ph); 7.84 (tr, 2H, ^3J = 7.32, H_{ortho} of Ph), 8.88 (dd, $^4J_{PH}$ = 14.88, $^3J_{PtH}$ = 19.35, =CH).

$^{13}C\{^1H\}$ NMR (C_6D_6, 25 °C) δ, ppm [J, Hz]: 15.55 (d, $^3J_{PC}$ = 7.28, CH_3); 61.23 (d,$^3J_{PtC}$ = 19.07, CH_2); 85.74 (s, C_5H_5); 124.95 (s, C_{para} of C_6H_5); 126.92 (s, C_{meta} of C_6H_5); 127.99 (s, C_{ortho} of C_6H_5); 142.29 (dd, $^3J_{PC}$ = 4.85, $^2J_{PtC}$ = 110.63, =C^2H), 142.85 (d, $^4J_{PC}$ = 9.36, C_{ipso} of C_6H_5); 196.41 (d, $^2J_{PC}$ = 1.73, Pt-CO); 227.42 (d, $^2J_{PC}$ = 3.47,μ-C^1 =).

$Cp(CO)_2RePt(\mu$-C=CHPh)[P(OPh)$_3$](CO) (3c) as a brown oil. Yield 80%.

Anal. Found: C, 43.38; H, 2.82%. Calc. for $C_{34}H_{26}O_6PPtRe$ (942.83): C, 43.31; H, 2.78.

IR (cm^{-1}): 2046 s, 1953 s, 1889 s (CH_2Cl_2); 2040 s, 1947 s, 1883 s (tabl. KBr).

^1H NMR (C_6D_6, 25 °C) δ, ppm [J, Hz]:5.11 (s, C_5H_5); 7.05–7.60 (H_{para},H_{meta},H_{ortho} of Ph); 8.84 (dd, $^4J_{PH}$ = 14.49, $^3J_{PtH}$ = 25.68, =CH).

$^{13}C\{^1H\}$ NMR (C_6D_6, 25 °C) δ, ppm [J, Hz]: 85.88 (s, C_5H_5); 121.25 (d, $^5J_{PC}$ = 5.55, C_{para} of OC_6H_5); 125.01 (s, C_{para} of C_6H_5);125.23(d, $^4J_{PC}$ = 1.04, C_{meta} of OC_6H_5);126.79(s, C_{meta} of C_6H_5); 127.90 (s, C_{ortho} of C_6H_5); 129.55 (s, C_{ortho} of OC_6H_5); 142.16 (dd, $^4J_{PC}$ = 9.36,$^3J_{PtC}$ = 19.25, C_{ipso} of C_6H_5); 142.76 (dd, $^3J_{PC}$ = 4.51,

$^2J_{PtC}$ = 104.39, =C^{2}H); 150.93 (dd, $^2J_{PC}$ = 5.89,$^3J_{PtC}$ = 10.23, C_{ipso} of OC_6H_5); 193.20 (dd, $^2J_{PC}$ = 2.43,J_{PtC} = 1231, Pt-CO); 200.79 (br, s, Re-CO); 227.68 (dd, $^2J_{PC}$ = 3.81,J_{PtC} = 867,μ-C^1 =).

4.3. X-ray diffraction studies of $Cp(CO)_2RePt(\mu\text{-}C{=}CHPh)[P(OPr^i)_3]_2$ (1a) and $Cp(CO)_2RePt(\mu\text{-}C{=}CHPh)[P(OPr^i)_3](PPh_3)$ (1b)

Crystal data and X-ray experimental details for complexes **1a** and **1b** are given in Table 3.

Orange crystals of μ$_2$-[(phenylethene-1,1-diyl-1:2κ^{2}C)]-dicarbonyl-1κ^{2}C-bis-(triisopropyl phosphite-2κP)-(1-η^5-cyclopentadienyl)-platinumrhenium(Pt-Re) (**1a**) suitable for X-ray diffraction analysis were grown from a hexane solution under argon atmosphere at +5 °C. Orange crystals of μ$_2$-[(phenylethene-1,1-diyl-1:2κ^{2}C)]-dicarbonyl-1κ^{2}C-(triisopropylphosphite-2κP)-(triphenylphosphane-2kP)-(1-η^5-cyclopentadienyl)-platinum–rhenium(Pt-Re) (**1b**) suitable for X-ray diffraction analysis were grown from a hexane:diethyl ether mixture = 2:1under argon atmosphere at +5 °C.

The experimental data were collected with an automatic Bruker X8 Apex diffractometer equipped with a two-dimensional CCD detector. The experimental completeness is 99.8% for both compounds. Absorption corrections (μ_{Mo} = 6.967 mm^{-1}) have been applied using multiscan procedure [53]. The supplementary crystallographic data for compound **1a** and **1b** have been deposited with the Cambridge Crystallographic Data Centre, CCDC No. 1957291, 1957292. The data can be obtained free of charge via http://www.ccdc.cam.ac.uk or e-mail: deposit@ccdc.cam.ac.u.

4.4. X-ray diffraction studies of $Cp(CO)_2RePt(\mu\text{-}C{=}CHPh)[P(OPr^i)_3](CO)$ (1c)

Crystal data and X-ray experimental details for complex **1c** are given in Table 3.

Orange crystals of μ$_2$-[(phenylethene-1,1-diyl-1:2κ^{2}C)]-tricarbonyl-1κ^{2}C,2κ^{1}C-(triisopropyl phosphite-2κP)-(1-η^5-cyclopentadienyl)-platinumrhenium(Pt-Re) (**1c**) suitable for X-ray diffraction analysis were grown from a hexane:diethyl ether mixture = 2:1 under argon atmosphere at +5 °C.

The experimental data were collected with a Smart Photon II diffractometer (Bruker AXS, CCD area detector, graphite monochromator). The experimental completeness is 99.8%. Absorption corrections (μ_{Mo} = 6.163 mm^{-1}) have been applied using multiscan procedure [54]. The structure was solved by direct methods and refined by full-matrix least squares on F^2, using SHELXTL program [55,56]. Hydrogen atoms have been placed in calculated positions and taken into account in the final stages of refinement in the “riding model” approximation. All hexa- and pentagonal cyclic groups were refined in idealized form. The supplementary crystallographic data for compound **1c** have been deposited with the Cambridge Crystallographic Data Centre, CCDC No. 1976304. The data can be obtained free of charge via http://www.ccdc.cam.ac.uk or e-mail: deposit@ccdc.cam.ac.uk.

CRediT authorship contribution statement

Oleg S. Chudin: Methodology, Investigation, Writing - original draft, Visualization. **Victor V. Verpekin:** Supervision, Conceptualization, Writing - original draft, Writing - review & editing. **Alexander A. Kondrasenko:** Data curation. **Galina V. Burmakina:** Writing - original draft, Data curation. **Dmitry A. Piryazev:** Data curation. **Alexander D. Vasiliev:** Data curation. **Nina I. Pavlenko:** Data curation. **Dmitry V. Zimonin:** Visualization, Data curation. **Anatoly I. Rubaylo:** Project administration, Funding acquisition.

Declaration of Competing Interest

The authors declare that they have no known competing financial interests or personal relationships that could have appeared to influence the work reported in this paper.

Acknowledgements

This work was conducted within the framework of the budget project AAAA-A17-117021310221-7 for Institute of Chemistry and Chemical Technology SB RAS using the equipment of Krasnoyarsk Regional Research Equipment Centre of SB RAS.

Appendix A. Supplementary data

Supplementary data to this article can be found online at https://doi.org/10.1016/j.ica.2020.119463.

References

[1] G. Gervasio, E. Sappa, A. Secco, J. Organomet. Chem. 751 (2014) 111–152.
[2] M. Akita, T. Koike, Dalt. Trans. 9226 (2008) 3523–3530.
[3] G. Sánchez-Cabrera, F.J. Zuno-Cruz, M.J. Rosales-Hoz, J. Clust. Sci. 25 (2014) 51–82.
[4] P. Buchwalter, J. Rosé, P. Braunstein, Chem. Rev. 115 (2015) 28–126.
[5] V. Ritleng, M.J. Chetcuti, Chem. Rev. 107 (2007) 797–858.
[6] R.J. Puddephatt, J. Organomet. Chem. 849–850 (2017) 268–278.
[7] N. Wheatley, P. Kalck, Chem. Rev. 99 (1999) 3379–3420.
[8] M.K. Karunananda, N.P. Mankad, J. Am. Chem. Soc. 137 (2015) 14598–14601.
[9] M. Böhmer, F. Kampert, T.T.Y. Tan, G. Guisado-Barrios, E. Peris, F.E. Hahn, Organometallics 37 (2018) 4092–4099.
[10] B.Y. Chor, W.X. Koh, R. Ganguly, Y. Li, L. Chen, R. Raja, W.K. Leong, J. Organomet. Chem. 849–850 (2017) 48–53.
[11] S. Sculfort, P. Braunstein, Chem. Soc. Rev. 40 (2011) 2741–2760.
[12] R.D. Adams, B. Captain, Angew. Chem. Int. Ed. 47 (2008) 252–257.
[13] J.M. Thomas, B.F.G. Johnson, R. Raja, G. Sankar, P.A. Midgley, Acc. Chem. Res. 36 (2003) 20–30.
[14] E.W. Abel, F.G.A. Stone, G. Wilkinson, Comprehensive Organometallic Chemistry: Heteronuclear Metal-Metal Bonds Vol. 10 Pergamon, 1995.
[15] A.S. Mohamed, I. Jourdain, M. Knorr, S. Boullanger, L. Brieger, C. Strohmann, J. Clust. Sci. 30 (2019) 1211–1225.
[16] L.S. Wang, M. Cowie, Organometallics 14 (1995) 2374–2386.
[17] J. Xiao, M. Cowie, Organometallics 12 (1993) 463–472.
[18] F.H. Antwi-Nsiah, O. Oke, M. Cowie, Organometallics 15 (1996) 506–520.
[19] M. Knorr, C. Strohmann, Eur. J. Inorg. Chem. (2000) 241–252.
[20] I. Jourdain, M. Knorr, C. Strohmann, C. Unkelbach, S. Rojo, P. Gomez-Iglesias, F. Villanfane, Organometallics 32 (2013) 5343–5359.
[21] M.E. Slaney, M.J. Ferguson, R. McDonald, M. Cowie, Organometallics 31 (2012) 1384–1396.
[22] T.J. MacDougall, R.G. Samant, S.J. Trepanier, M.J. Ferguson, R. McDonald, M. Cowie, Organometallics 31 (2012) 1857–1869.
[23] K. Uehara, S. Hikichi, M. Akita, Chem. Lett. 31 (2002) 1198–1199.
[24] M. Knorr, I. Jourdain, Coord. Chem. Rev. 350 (2017) 217–247.
[25] A.B. Antonova, Coord. Chem. Rev. 251 (2007) 1521–1560.
[26] H. Werner, J. Wolf, G. Müller, C. Krüger, Angew. Chem. Int. Ed. English 23 (1984) 431–432.
[27] N.E. Kolobova, L.L. Ivanov, O.S. Zhvanko, G.G. Aleksandrov, Y.T. Struchkov, J. Organomet. Chem. 228 (1982) 265–272.
[28] N.E. Kolobova, L.L. Ivanov, O.S. Zhvanko, A.S. Batsanov, Y.T. Struchkov, J. Organomet. Chem. 279 (1985) 419–432.
[29] H. Werner, F.J.G. Alonso, H. Otto, K. Peters, H.G. Von Schnering, J. Organomet. Chem. 289 (1985) c5–c12.
[30] M.I. Bruce, Chem. Rev. 91 (1991) 197–257.
[31] H. Werner, F.J.G. Alonso, H. Otto, K. Peters, H.G. Von Schnering, Chem. Ber. 121 (1988) 1565–1573.
[32] A.B. Antonova, S.V. Kovalenko, E.D. Petrovsky, G.R. Gulbis, A.A. Johansson, Inorganica Chim. Acta 96 (1985) 1–7.
[33] A.B. Antonova, S.V. Kovalenko, E.D. Korniyets, P.V. Petrovsky, A.A. Johansson, N.A. Deykhina, Inorganica Chim. Acta 105 (1985) 153–163.
[34] A.B. Antonova, S.V. Kovalenko, A.A. Johansson, E.D. Korniyets, I.A. Sukhina, A.G. Ginzburg, P.V. Petrovskii, Inorganica Chim. Acta 182 (1991) 49–54.
[35] A.B. Antonova, O.S. Chudin, A.D. Vasiliev, N.I. Pavlenko, W.A. Sokolenko, A.I. Rubaylo, O.V. Semeikin, J. Organomet. Chem. 694 (2009) 127–130.
[36] A.B. Antonova, O.S. Chudin, N.I. Pavlenko, W.A. Sokolenko, A.I. Rubaylo, A.D. Vasiliev, V.V. Verpekin, O.V. Semeikin, Russ. Chem. Bull. Int. Ed. 58 (2009) 955–963.
[37] A.B. Antonova, V.V. Verpekin, O.S. Chudin, A.D. Vasiliev, N.I. Pavlenko, W.A. Sokolenko, A.I. Rubaylo, O.V. Semeikin, Inorganica Chim. Acta 394 (2013) 328–336.
[38] V.V. Verpekin, A.A. Kondrasenko, O.S. Chudin, A.D. Vasiliev, G.V. Burmakina, N.I. Pavlenko, A.I. Rubaylo, J. Organomet. Chem. 770 (2014) 42–50.
[39] V.V. Verpekin, A.D. Vasiliev, A.A. Kondrasenko, G.V. Burmakina, O.S. Chudin, N.I. Pavlenko, D.V. Zimonin, A.I. Rubaylo, J. Mol. Struct. 1163 (2018).

[40] K.I. Utegenov, V.V. Krivykh, O.S. Chudin, A.F. Smol'yakov, F.M. Dolgushin, O.V. Semeikin, N.A. Shteltser, N.A. Ustynyuk, J. Organomet. Chem. 867 (2018) 113–124.
[41] P.S. Pregosin, S.N. Sze, Helv. Chim. Acta 60 (1977) 1371–1375.
[42] O.A. Gansow, A.R. Burke, W.D. Vernon, J. Am. Chem. Soc. 98 (1976) 5817–5826.
[43] J.M. Anna, J.T. King, K.J. Kubarych, Inorg. Chem. 50 (2011) 9273–9283.
[44] J.C. Jeffery, H. Razay, F.G.A. Stone, J. Chem. Soc., Dalt. Trans. (1982) 1733–1739.
[45] M. Berry, J.A.K. Howard, F.G.A. Stone, J. Chem. Soc., Dalt. Trans. (1980) 1601–1608.
[46] A.B. Antonova, O.S. Chudin, N.I. Pavlenko, W.A. Sokolenko, A.I. Rubaylo, A.D. Vasiliev, V.V. Verpekin, O.V. Semeikin, Russ. Chem. Bull. 58 (2009).
[47] B. Cordero, V. Gómez, A.E. Platero-Prats, M. Revés, J. Echeverría, E. Cremades, F. Barragán, S. Alvarez, Dalt. Trans. (2008) 2832.
[48] G.V. Burmakina, V.V. Verpekin, O.S. Chudin, D.V. Zimonin, N.I. Pavlenko, A.B. Antonova, A.I. Rubaylo, J. Sib. Fed. Univ. Chem. 1 (2013) 51–59.
[49] D.A. Valyaev, O.V. Semeikin, M.G. Peterleitner, Y.A. Borisov, V.N. Khrustalev, A.M. Mazhuga, E.V. Kremer, N.A. Ustynyuk, J. Organomet. Chem. 689 (2004) 3837–3846.
[50] L.N. Novikova, M.G. Peterleitner, K.A. Sevumyan, O.V. Semeikin, D.A. Valyaev, N.A. Ustynyuk, V.N. Khrustalev, L.N. Kuleshova, M.Y. Antipin, J. Organomet. Chem. 631 (2001) 47–53.
[51] G.V. Burmakina, V.V. Verpekin, N.G. Maksimov, D.V. Zimonin, D.A. Piryazev, O.S. Chudin, A.I. Rubaylo, Inorganica Chim. Acta 463 (2017).
[52] A.H. Ford-Moore, B.J. Perry, Org. Synth. 31 (1951) 111.
[53] G.M. Sheldrick, 1997.
[54] G.M. Sheldrick, V. Sadabs, Madison, Wisconsin, USA, 2004.
[55] G.M. Sheldrick, Acta Crystallogr. Sect. A Found. Adv. 71 (2015) 3–8.
[56] G.M. Sheldrick, Acta Crystallogr. Sect. C Struct. Chem. 71 (2015) 3–8.